PERFORMANCE EVALUATION OF THIN WALLED TUBE FILLED WITH NANO BASED POLYURETHANE RIGID FOAM FOR INCREASED ROOF STRENGTH OF A VEHICLE

A Thesis by

Anush Kumar Malli

Bachelor of Engineering, Jawaharlal Nehru Technological University, 2008

Submitted to the Department of Mechanical Engineering

and the faculty of Graduate School of

Wichita State University

in partial fulfillment of

the requirements for the degree of

Master of Science

July 2012

PERFORMANCE EVALUATION OF THIN WALLED TUBE FILLED WITH NANO BASED POLYURETHANE RIGID FOAM FOR INCREASED ROOF STRENGTH OF A VEHICLE

The following faculty members have examined the final copy of this thesis report content, and recommend that it can be accepted in partial fulfillment of the requirements for the degree of Master of Science with a major in Mechanical Engineering.

_____

Hamid M Lankarani, Committee Chair

_____

Krishna Krishnan, Committee Member

_____

Michael McCoy, Committee Member

DEDICATION

To my Family and Advisor

ACKNOWLEDGEMENTS

I take this opportunity to thank every individual who made this thesis possible. Firstly, I wish to express my deepest and sincere gratitude to my advisor Dr. Hamid M. Lankarani. I am amazingly fortunate to have an advisor who gave me the freedom to explore on my own and helped me to prosper and achieve the most important goals of my career. His understanding and scholarly support helped me overcome many crisis situations during my journey at Wichita State University. Without his support and guidance, this thesis would not have been possible.

I extend my gratitude and appreciation to my committee members, Dr. Krishna Krishnan and Dr. Michael McCoy for their time and effort in reviewing this manuscript.

I am very thankful to my friends Sachin Patil, Kranthi Pingili, Damodar Tankara, Sandeep Gadiparthi, Manikanta Bijju, Vinay Adigoppula, Shravan Sabbani, Rajarshi Setpally, Lakshmi Koneru, Bhujanga Adapa, for extending their helping hand during my thesis and also to the ones who helped me stay sane in my difficult times. I greatly value their friendship and deeply appreciate their concern and support at all times.

I would also like to extend a special note of thanks to my friend Rasoul Moradi for his valuable comments and suggestions. His help and effort in guiding me even during his busy schedules were truly appreciable.

I express my heart-felt gratitude to my beloved parents and my brothers Dinesh and Abhilash. I am always grateful for their constant support and encouragement at every phase of my life. Their love and prayers kept me healthy and prosperous.

Finally, I would like to thank the faculty and staff of Department of Mechanical Engineering for the support and guidance throughout my graduate studies and Wichita State University for giving the best and wonderful moments to cherish in life.

ABSTRACT

Automotive crash has garnered significant attention in the recent years with increasing fatality and safety concerns. Substantial effort and great amount of time and expertise has been directed towards the issues related to crashworthiness such as impact, rollover scenarios and restraint performance. Automotive rollover is one of those important concerns for the auto industry as the fatality rates and death causing conditions are vital compared to other crashes. In the past few decades, research has been focused towards developing efficient roof structure by implementing crashworthy structures, to protect or at least reduce the severity of the accident to the occupants of the vehicle during an event of a rollover. Studies have been carried in this area in developing efficient crashworthy structures.

As the technology is evolving, researchers have found that thin walled tubes filled with foam materials possess high energy absorption properties compared to empty crashworthy structures. Further research in this has area led to the interference of nanotechnology, which implements emerging techniques in developing advanced materials for engineering applications. Scientists were able to develop low density, lightweight foams with high energy-absorption characteristics with these techniques.

The purpose of this thesis is to analyze and evaluate the performance of low density carbon nanofoam (CNF) as an energy absorbing material in improving the roof strength of the vehicle. The LS-DYNA code, a non-linear dynamic finite element solver is utilized to accomplish this study. First, a three-point bending test simulation is carried as component level testing to analyze the behavior of foam materials. Then, the energy absorbing characteristics of a hollow tube is studied and the results are compared with regular polyurethane (PU) foam and carbon nanofoam inserts into the hollow tube, under similar conditions. Finally, PU foam and CNF is applied into the critical areas of roof supporting structures as two different conditions and static roof crush and dynamic inverted drop test simulations are conducted depicting an actual rollover scenario to study the crashworthy behavior of the vehicle roof with and without the foam.

This study highlights that carbon nanofoam is found to be more effective compared to the regular polyurethane foam exhibiting better energy absorption characteristics.

TABLE OF CONTENTS

Chapter **Page**

TABLE OF CONTENTS (Continued)

Chapter **Page**

LIST OF FIGURES

Figure **Page**

LIST OF FIGURES (Continued)

Figure **Page**

LIST OF FIGURES (Continued)

Figure **Page**

LIST OF TABLES

Table **Page**

CHAPTER 1

INTRODUCTION

1.1 Automobile and Crashworthiness

The evolution of automobile played a vital role in the history of mankind, making its mark as one of the greatest achievements and one of the biggest revolutions in transportation industry. It also made life of human easier and comfortable. Science and technology has been a major contributor for the growth of automotive technology and increase in growth and demand for the auto industry. The advancement of automotive technology is leading to new innovations and developments ever since the evolution. As the automobile is growing its importance at a very fast pace, concerns regarding the safety of the driver and passengers inside the car has also been increasing. There are different types of accidents which include front, rear and side impacts and rollover in which the loads are distributed symmetrically or non-symmetrically with respect to vehicle body and cause severe to death causing injuries to the occupants of the vehicle.

The increase in fatalities or deaths due to vehicle accidents has drawn a great deal of attention for safety of occupants of the vehicle. Special efforts have been made by several engineers and researchers around the globe in developing safe theoretical design criteria on mechanics of crumpling in designing safe vehicle structures. They came up with new ideas and techniques to reduce or minimize the severity of crash by optimizing or developing crashworthy structures inside of the car. These structures help in reducing or eliminating the effects of the impact on the occupants. This ability of a structure to protect its occupants during an impact is called “crashworthiness”.

The vehicle body is considered crashworthy if it deforms in a controlled manner, absorbing the maximum kinetic energy imposed by the impact while maintaining adequate or sufficient residual space around the passengers, so that auxiliary restraining devices can reduce the body collision [1]. Crashworthiness has been receiving a great deal of attention all over the world due to the concerns of safety of the occupants in the car. Great amount of time and expertise has been directed towards this field, to provide safe and crashworthy structure.

1.2 Crashworthy Tubes and Collapse Mechanism

The design of vehicle structures is very important to prevent or reduce the severity of accidents or impacts during a crash. Different structures such as shells, tubes, stiffeners and sandwich panels have been identified as efficient energy absorbing systems in a vehicle, also termed as "energy absorbers". Therefore, extensive research has been carried over decades to improve the energy absorption characteristics of such materials. These structures made of ductile materials are subjected to different loadings and a wide range of deformation such as compression or flattening, axial or flexural bending. Due to good energy absorption characteristics, tubular structures or crashworthy tubes have been widely used in different engineering applications as structural members, largely in the transportation industry for vehicle structural design.

The collapsible behavior of these crashworthy tubes has been one of the main areas of concentration in automotive industry due to their energy absorption characteristics. Several attempts were made by researchers and engineers around the globe to understand the energy absorption characteristics and the crushing behavior of these structural members. In general, the study of deformation in these structural energy absorbers accounts for geometrical shape, mode of collapse, strain hardening and strain rate effect [2]. There are several approaches to study the energy absorption or collapse mechanism of the structural members such as finite element analysis, experimental and theoretical analysis. Theoretical Analysis approach is generally considered as early or basic approach since it is relatively simple and fast. Theoretical analysis of the collapse mechanism is determined using plastic – hinge method. Where, thin walled members when crushed by any load, the collapse strength is reached and plastic deformations are occurred over the folding lines called hinge lines [2]. The local or global collapse will progress when these hinge lines are formed around the structure and the internal energy of the structure is determined by the hinge line plastic deformation. This mechanism is also known as rigid plastic collapse mechanism.

The comparison of analytical and experimental results usually gives a better understanding of a closed form solution of thin walled circular tube subjected to bending. The collapse mechanism of tube

bending is generally categorized into three different phases i.e., elastic behavior, ovalisation plateau and structural collapse [2].

1. Elastic behavior
2. Ovalisation plateau
3. Structural collapse

1.2.1 Elastic behavior

The elastic behavior of the structure can be determined as the linear increase in the moment with constant slope to yield moment- rotation. It can be shown as [2]:

$$M_y = \frac{2\sigma_y I}{D_0} \tag{1.1}$$

$$\theta_y = \frac{M_y L_0}{EI} \tag{1.2}$$

Where, M_y is the yield moment, L_0 is pure moment length, E is the elastic modulus, I is Second moment of area, σ_y is the measured yield stress, θ_y is the yield rotation angle and D_0 is outside diameter of the tube

1.2.2 Ovalisation plateau

In this phase, the material exhibits slight hardening and the circular cross section undergoes slight ovalisation when subjected to bending. During the increment of bending rotation, the bending moment is generally constant. The ultimate moment of the tube at ovalisation is given by [2].

$$M_{ovalised} = S_{ovalised}\sigma_y = \frac{4}{3}(R_v^2 R_h - R_{vi}^2 R_{hi})\sigma_y \tag{1.3}$$

Where, $S_{ovalised}$ is the plastic section modulus of the tube, σ_y is the yield stress of the ovalised tube, R_h and R_v are the horizontal and vertical radii of the ovalised tube

Here,

$$R_h = \frac{D_h}{2} = 0.55D_0 \ , \ R_v = \frac{D_v}{2} = 0.45D_0 \tag{1.4}$$

The Horizontal and vertical diameter D_h and D_v are shown in Figure 1.1.

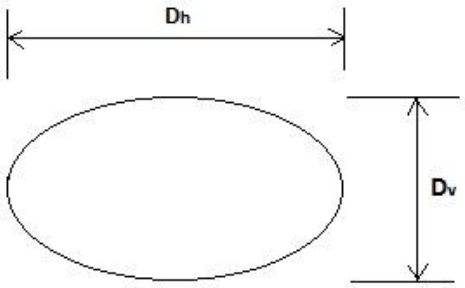

Figure 1.1 Horizontal and Vertical Diameter of the Ovalised Tube [2]

1.2.3 Structural collapse

This is the final phase of the collapse mechanism of tube bending. In this phase, the load carrying capacity of the structure decreases at a very high pace. As shown in Figure 1.1, the plastic folding of the tube is being deformed in the plastic zone and the model involves the hinge flattened at the circumferential cross section. The oblique hinge lines can be observed along the length of the tube. The line connecting points A and B, shown in Figure 1.2 is for the traveling hinges of the flattened region in the circumferential cross section. The rolling hinge with radius r and the circular arc of radius R_1 determines the four oblique hinge lines along the longitudinal tube the length of the plastic zone denoted by H.

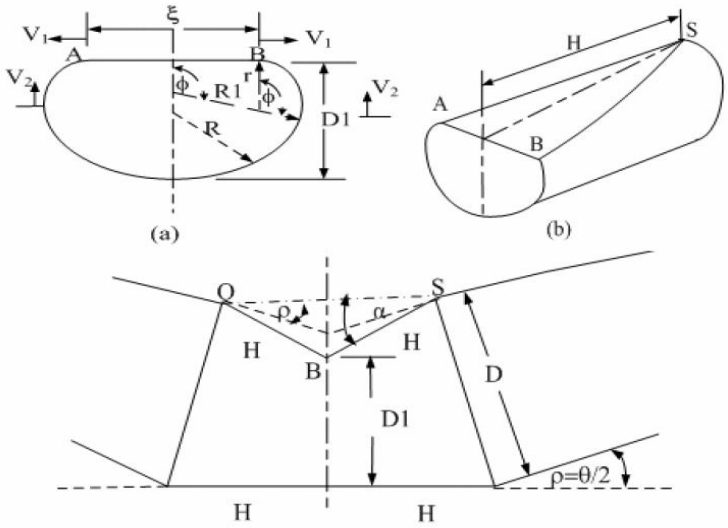

Figure 1.2 Dimensional Parameters of a Structural Collapse Mechanism [2]

1.3 Different Load Classification of Tubular Structures

In engineering applications or different structural analysis, loads are classified with respect to rising time or loading of the mechanical system. Depending on these factors, there are four types of loadings: static loading, fatigue loading, Dynamic loading and Impact loading. As shown in Figure 1.3, when a mechanical system is subjected to loading (P), the load is assumed to be linear until it reaches the maximum loading and the time taken by the load to reach its maximum limit determines the type of loading of that particular system.

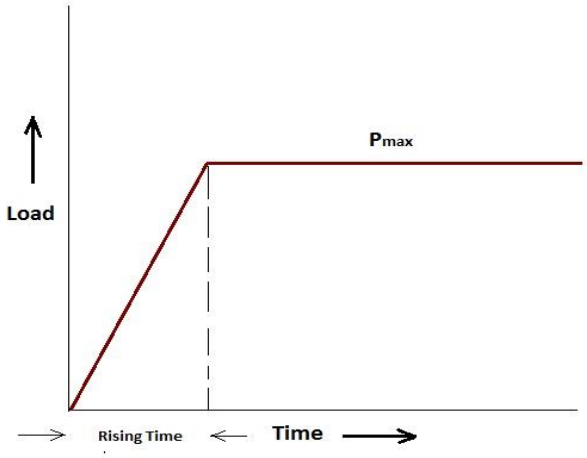

Figure 1.3 Typical Load vs Time Curve

1.3.1 Static loading

Static load is defined as a load where the rising time is three times more than that of the original time period of the mechanical system. In a static loading the load acts constant with respect to time. In general this type of loading is carried out to determine the stress, strain relation or the load verses displacement characteristics of a material.

1.3.2 Fatigue loading

Fatigue loading is similar to static loading. The basic difference between the both is that the variation of load with respect to time remains constant, also load varies with respect to time. Moreover, the static rise time of the load is three times the fundamental period.

1.3.3 Impact loading

In this type loading, the fundamental time period is 0.5 times the rise time loading of the mechanical system. In general these types of loading are destructive type and are one of the expensive types of experimental study, as the equipment or set up are expensive. The study of these types of loadings is considered to be important and accurate.

Due to these disadvantages or drawbacks, the finite element analyses are considered to be an alternative method to represent the experimental impact tests numerically in simulations. The main advantage with finite element analysis of impact tests is that, the errors can be corrected easily with very less effort compared to that of the experimental set up and also it is less expensive and requires very less man power.

1.3.4 Dynamic loading

In dynamic loading, the rise time usually ranges between 1.5 to 3 times of the fundamental time (Tn) of the mechanical system. This type of loadings are mainly used for stress and displacement study

1.4 Factors Affecting Behavior of Tubular Structures

There are different testing methods to study and determine the behavior of tubular structures numerically or experimentally. Depending on the requirement and the type of application, a particular method is used. One such method which is widely used to study the energy absorption characteristics or the flexural stiffness of the material is the flexural testing method. It is also commonly known as 3- point or 4- point bending or flex method. The flexural test method helps in determining the behavior of materials which are subjected to simple beam loading. In general, the specimen undergoes two different shapes, when performing a flex test i.e., concave shape and convex shape producing tensile stress in the convex side and compression stress in the concave side. Figure 1.4 shows the general setup of a 3- point bending machine.

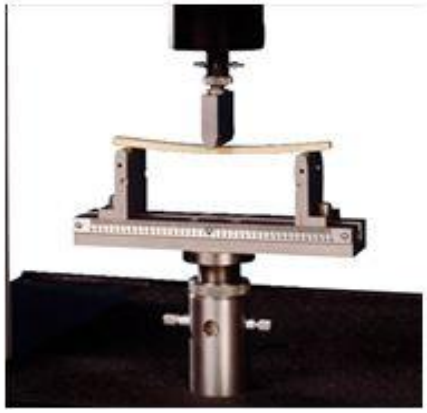

Figure 1.4 INSTRON 2810 Bending Machine [3]

When conducting a three point bend test of a hollow tube, different factors are to be considered such as deflections in the specimen, stress and strain in the beams and applied load to the tube. All these factors help in studying the material behavior of hollow tube.

1.4.1 Stress and strain

Stress is defined as the load per unit area or internal forces acting during the process of deformation of a body or material and is determined by:

$$\sigma = \frac{P}{A} \tag{1.5}$$

When conducting a three point flexural testing, the flexural stress σ_f can be determined as [23]:

$$\sigma_f = \frac{3PL}{2bd^2} \tag{1.6}$$

Where, P is load at given point, L is length of span, R is radius of the tube, A is the area of cross-section

Strain is the deformation or change in shape of the material under applied forces. It is shown as

$$\varepsilon = \frac{\delta}{l} \tag{1.7}$$

When conducting a bend test, the flexural strain is determined ε_f as [23]:

$$\varepsilon_f = \frac{6Dd}{L^2} \tag{1.8}$$

Where, D is maximum deflection at center of the beam, d is depth of the beam, L is support span

The strain during bending can be calculated using simple strain gauges; the bending stress is calculated based on bending moment at that particular strain gauge location and the distance from centroidal or neutral axis. The strain at certain angle θ corresponding to the strain gauge orientation is determined by the rotation of coordinate system. This transformation can be shown as [23]:

$$\varepsilon_\theta = \varepsilon_x \cos^2\theta + \varepsilon_y \sin^2\theta + \gamma_{xy} \sin\theta\cos\theta \tag{1.9}$$

Where, ε_x, ε_y and γ_{xy} are predicted strains.

1.4.2 Free body diagram for applied load:

A free body diagram is always a better way to understand and solve a problem analytically as shown in Figure 1.5. In our case, for a bending of a tube, the load applied on each beam can be solved by equations of static equilibrium and force at the load cell.

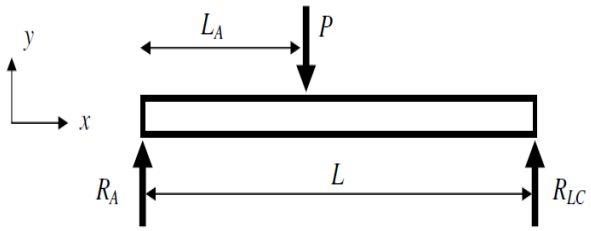

Figure 1.5 Free Body diagram of a Tube Bending [23]

The applied load P on the beam can be calculated by the sum of moments at A [23]:

$$\Sigma M_A = 0 = -PL_A + R_{LC}L \tag{1.10}$$

To calculate the reaction force at A, the sum of forces in the y direction is given by [23]:

$$\Sigma F_y = 0 = R_A - P + R_{LC} \tag{1.11}$$

To calculate the Centroid and moment of inertia, the dimensions of beam cross section is being considered. The position in y-direction of the centroid from the bottom of the round tube is:

$$\bar{y} = \frac{D_0}{2} \tag{1.12}$$

The moment of inertia about the z-axis is given by [23]:

$$I_z = \frac{\pi}{64}(D_o^4 - D_i^4) \tag{1.13}$$

Here, D_o is Outer diameter of the round tube, D_i is the inner diameter of the round tube

The maximum deflection when the tube is subjected to bending can be determined by Euler-Bernoulli beam theory [23]:

$$\delta_{theory} = -PL_A^2(L - L_A)^2 / 3EI_z L \tag{1.14}$$

1.4.3 Hooke's law

The predicted stress and strain in beams can be calculated using Hooke's Law. It states that within the elastic limit of a solid material deformation, stress is directly proportional to strain. Neglecting shear force effect on the beams, the stresses at that strain gauge are only due to bending [23].

$$\sigma_x = \frac{My}{I_z}, \sigma_y = 0, \tau_{xy} = 0 \tag{1.15}$$

Where, M is the moment induced due to applied load and length of the beam.

The normal and strain due to shear are given can be determined using Hooke's law [23]:

$$\varepsilon_x = \frac{1}{E}[\sigma_x - \nu(\sigma_y + \sigma_z)], \quad \varepsilon_y = \frac{1}{E}[\sigma_y - \nu(\sigma_x + \sigma_z)] \tag{1.16}$$

$$\gamma_{xy} = \frac{\tau_{xy}}{G} \tag{1.17}$$

1.4.4 Energy absorption

The total energy absorbed by a tubular structure before the failure is shown as:

$$E_t = \int_0^{U_t} F du \tag{1.18}$$

Where, F is the bending force, υ is the displacement of the Indenter, υ_f is the displacement of the Indenter at failure of the structure.

The mass efficiency of the energy absorption for a structure is defined as:

$$E_S = \frac{E_t}{M_t} \tag{1.19}$$

Where, m_t is total mass of the structure

1.5 Rollover Accidents

Auto accidents have been a great concern in the transportation industry. As the numbers of vehicles are increasing every year globally, the number of occupant injuries and deaths due to the vehicular crashes are increasing as well. There are nearly 6,000,000 auto accidents every year accounting for 115 deaths every day in vehicle crashes in United States, one death for every 13 minutes [6].

According to National Center of Health (NCH) statistics in 2005, the vehicular accidents are among the major causes of deaths in the United States. It is clearly established that vehicular accidents have a significant contribution in the number of deaths in population every year. Researchers and automotive engineers in the industry throughout the globe are challenged to design and develop safer and crashworthy vehicles due to the raising concern of auto accidents globally. Table 1.1 shows the rate of deaths per 100,000 standard populations.

Table 1.1 Causes of deaths per 100,000 U.S standard populations according to centers for disease control and prevention according to NHTSA, 2005 [5]

Causes	**2005**	**2004**
Diseases of heart	210.3	217.0
Malignant neoplasms	183.8	185.8
Cerebrovascular diseases	46.6	50.0
Diabetes Mellitus	24.5	24.5
Alzheimer's disease	22.9	21.8
Vehicular accidents	**14.7**	**14.6**
Septicemia	11.2	11.2
Intentional self-harm (suicide)	10.6	10.9
Chronic liver disease and cirrhosos	8.9	9.0
Assault (homicide)	5.9	5.9

Of all the vehicular accidents, rollover accidents are the most complex and least understood due to the complexity of phenomenon involved even though it is not the most frequent type of accident. Study towards rollover accidents has greatest significance in the auto industry due to the trauma caused to the vehicle occupants during the crash [5]. It has become an important concern in recent years especially for vehicles with high center of gravity such as SUV's and trucks. These rollover crashes are considered to be the dangerous incidents due to higher fatality rate compared to other auto crashes. According to NHTSA's statistics and analysis from 1991-2001, the number of passenger vehicle occupants deaths due to auto crashes increased 4 percent while fatalities in rollover accidents increased 10 percent. In 2001 alone 10,138 people died in the rollover crashes [4]. The most recent statistics from Insurance Institute of Highway Safety (IIHS) 9023 people died due to the rollover accidents in 2008. Figure 1.6 shows a typical rollover accident of an SUV and the occupant response during the rollover event.

Figure 1.6 Rollover Accidents and Effect to Driver inside the Vehicle [12]

Although rollover accidents are less than 4 percent of all motor vehicle accidents, it accounts for more than a third of passenger deaths or more than 20 percent of total occupant deaths in the vehicular accidents [5]. According to report from NHTSA in 2005, 3.3 percent of rollover accidents are being determined in which the fatality rate was 21.2 percent. The statistics are shown in Figure 1.7.

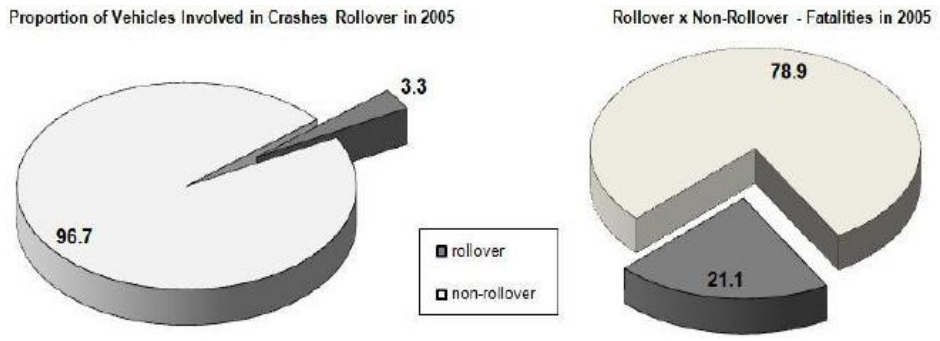

Figure 1.7 Proportions of Vehicles Involved in Rollover and Fatalities According to NHTSA 2005 [5]

Researchers with extensive study determined that most of the fatalities or severe injuries due to the rollover are associated with the roof intrusion in to the occupant zone of the vehicle during the crash. They are coming up with new ideas and innovations to improve the roof strength and reduce or minimize the injuries to the occupants inside the vehicle during a rollover. Some of the improvements to minimize these types of accidents are:

- Improving vehicle design and maintenance
- Introducing roll bars and cages into the body structure of the vehicle.
- Implementing air bags at crucial areas inside the vehicle.
- Improving the material strength of the structure
- Introducing foam materials inside the hollow structures of the vehicle body to minimize the intrusion of the metal into the vehicle during a crash or accident.

1.6 The Physics of a Rollover Accident

Rollover is a type of vehicle accident where the vehicle tips on to the side or the roof. There are several ways, where a rollover can occur which include excessive cornering speed, tripping, passing across a critical slope or collision with another vehicle. Every rollover undergoes three basic phases: The loss of control phase, the tripping phase and rollover or tumbling phase [9]. In simple physics, vehicles with narrow track width and high center of gravity are prone to rollover than vehicles with wider track width and low center of gravity. Altering either of the factors can minimize this effect such as lowering

the center of gravity or widening the track width of the vehicle. Figure 1.8 shows the CG and track width of a vehicle.

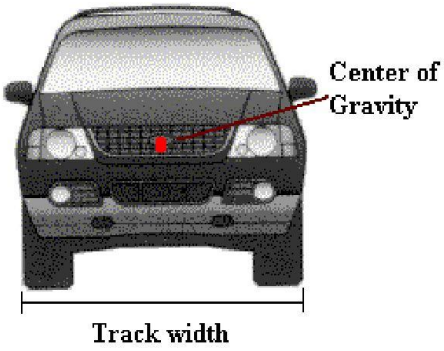

Figure 1.8 CG and Track Width of a Vehicle [8]

According to Newton's first law, when a vehicle is making a turn or a round, it wants to go straight but the tires creates a 'lateral centripetal force' or central force, caused due to the friction between the tires and the road to make a turn. At this point, the vehicle experiences different forces like gravity, inertial forces and forces due to the friction. When a vehicle is making a turn, the frictional force acts between the tire and the road being in the direction of turn, there is an another force acting on the vehicle opposite to the forces of friction called 'Centrifugal force' which is caused by the inertia of the body. This force helps in stabilizing or drawing the vehicle away from the center of rotation and opposite to centripetal force, supporting the Newton's first law of motion in this condition. The centrifugal force can be defined as an apparent force equal and opposite to the centripetal force caused by the inertia of a body drawing the body away from the center of rotation. This phenomenon is shown in Figure 1.9.

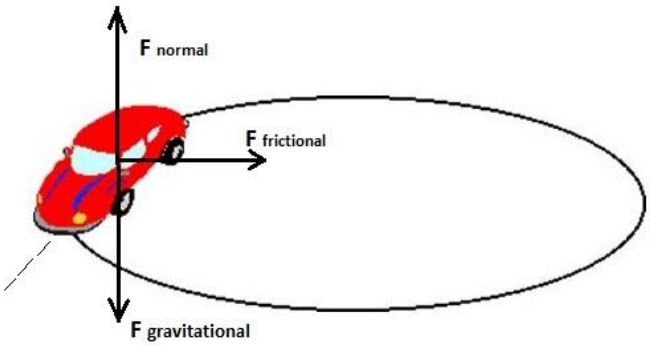

Figure 1.9 Various Forces Acting on a Vehicle when making a Turn

In a situation where the vehicle is making a turn and the road is slippery, the friction between the tires and the road is low, reducing the coefficient of friction or not enough static coefficient of friction and causing the vehicle to skid forward. At the same time if the tires are locked up, the coefficient of friction is increased to a point where the centripetal force becomes greater than the centrifugal force giving more scope or causing a vehicle to rollover.

In general the force acting on the vehicle when turning or in a curved motion is represented by F=ma. For example, when a vehicle is making a right turn, the force due to the tire- road friction and centrifugal force of the vehicle act in opposite directions as shown in Figure 1.10 which is relevant to the condition of the vehicle moving in a straight direction according to the Newton's law. At this scenario, the occupant inside is also moving forward but feels like force drawing him to left side as it is due to the centrifugal force of the vehicle.

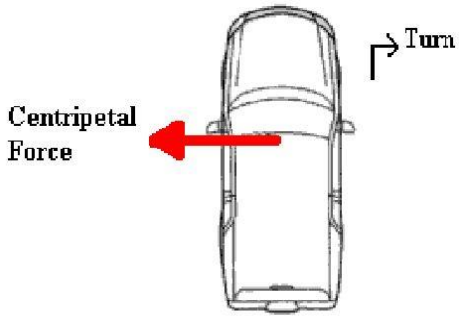

Figure 1.10 Centripetal forces acting on a vehicle when making a turn [8]

The force exerted on the vehicle due to tire road frictional force in circular motion is represented as [8]

$$F = (W \times v \times v) / (g \times r) \tag{1.20}$$

Where, W is weight of the vehicle, v is velocity/ speed, r is radius of the circle, g is acceleration due to gravity

Generally, every material body has a fixed point at its center through which the resultant force of gravitational attraction acts. This point is often called as the Center of gravity. It is the line through the length of the vehicle on which the entire vehicle can be balanced [8]. When a vehicle is making a turn,

there is always identical force acting at the center of gravity which would also represent the centripetal force acting on the vehicle by road. The identical force is equal and opposite to the centripetal force drawing at a height of bottom of the tires. This would be analyzable as both translational and rotational effects [8]. This can be clearly shown in Figure 1.11.

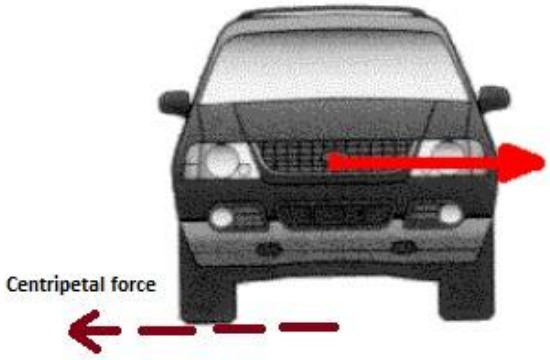

Figure 1.11 Centripetal and Opposite Equal Force acting on the Vehicle [8]

There are two different component forces acting upon the body especially when making a turn shown in Figure 1.12. One component force is directed towards the thread of the tire. This is resultant force acting at the tire thread (friction between tire and the road), which gives sideways forces to the vehicle especially when making a turn, determining that tire threads can transfer sideway forces to the vehicle to turn corners. Similarly, the second component force acting at right angles between CG and tire thread is directed up and outward which tries to roll over the vehicle around the outer tire thread [8].

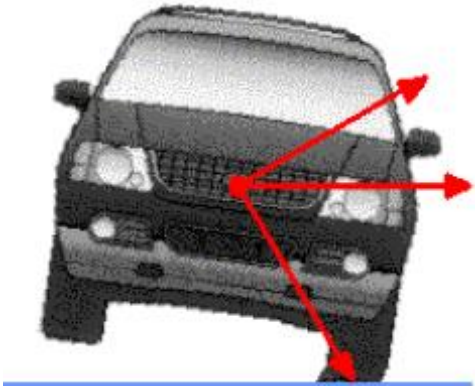

Figure 1.12 Different Component Forces acting on a Vehicle during Rollover [8]

So when making a quick or sharp turn, the center of gravity goes higher and the static coefficient of friction between the tires and the road is reduced tremendously, causing the tire to lose contact with the road making the vehicle to tilt and raised up. This gives more scope for the component forces to act spontaneously as discussed above.

1.7 Motivation and Objectives

A significant number of people are killed or injured in auto accidents ever year, in which the fatalities are significant in rollover accidents compared to other auto accidents such as frontal, rear and side impacts. The most recent accident statistics provided by IIHS show that high percentage of fatalities due to auto accidents are due to rollover with 9023 deaths in the year 2008 [6].

The foam materials have gained more attention in automotive industry during the recent years. Due to their high energy absorbing characteristics and good mechanical and thermal properties, foams are used in various structural applications in an automobile for safety concerns. Foams are being used for various applications such as:

- In bumpers for energy absorption during frontal, rear impact and pedestrian protection.
- In doors for side impact protection and also used as padding materials in different parts of vehicle.
- In railings for energy absorption during a crash.
- Under steering columns to protect the driver knees during an accident.
- Behind the head liners for head impact protection.

The present study of foam infusion into the hollow crashworthy tubes of the vehicle comes from this ideology.

The aim of this research is to analyze the energy absorption characteristics of a thin walled tube in bending with and without foam insert. The individual objectives of this research are:

- To conduct a study on foams that are being used as core materials for energy absorption applications in thin walled tubes and the effect of infusion of carbon nanoparticles into the polyurethane will be studied.
- To carry out a component level bending test simulation on a thin walled tube to examine the energy absorption characteristics.
- To conduct a study on three different bending test conditions ie, Hollow tube, tube with PU foam insert and tube with Carbon nanofoam insert.
- To introduce the foam into A- pillar, B- pillar and Roof Header and Roof side rail of a Ford Explorer and investigate its effect on energy absorption capacity for increase in roof strength.
- To conduct a Quasi – Static (FMVSS 216) and Dynamic roof crush (SAE J996) analysis on the vehicle to study the variation in roof strength.

CHAPTER 2

LITERATURE REVIEW

2.1 Introduction

In automotive industry, crashworthiness is defined as a measure of the ability of a structure to plastically deform yet maintaining a sufficient space of survival for the occupants inside the vehicle during crashes involving practical deceleration loads. The secondary purpose is to reduce the damage to the vehicle.

Generally, an excessive stiff structure is considered to be favorable against deformation but it also reduces the crashworthiness, as it increases the rate of occupant injury during severe impacts. Due to this concern, a structure is supposed to be stiff at certain portions to prevent intrusions into the sensitive areas of the passenger compartment and soft in some regions to absorb the forces before it reaches the stiffened regions. This can be easily achieved by regulating the crushing behavior of these structural parts and placing energy absorbing components in areas prone to accidents. Figure 2.1 shows the typical energy absorbing structures of a car.

Figure 2.1 Typical Energy Absorbing Structures of a Car [13]

Passenger vehicle crashworthiness has gained significance importance in the recent years. According to NHTSA, over six million vehicle crashes were reported in United States in the year 2000, claiming more than 40000 deaths [6], Out of which the fatality rate is more in rollover accidents.

An automobile is designed to meet several impact scenarios such as frontal, side, rear impact and rollover, of which rollover is one of the important concern for any crash engineer. Steel countermeasures are typically used as structural reinforcing elements to the structure of the body to improve vehicle roof crush strength during a rollover scenario [11]. Most of these structural elements of the vehicle are thin walled tubes, which undergo deformation due to buckling, crushing and bending. These thin walled tubes are also called as crashworthy tubes. As the crushing load is applied at the proximal end of the tube, the distal end supported by a strong structure undergoes deformation depending on the nature of crushing force. This type of loading is similar to compression and bending under quasi static condition. The stability of these tubes is equally important as its mean crushing force and energy absorption [7].

Researchers conducted several experiments to improve the crash resistance and energy absorption of these structural elements, studying the cross sections of different thin walled tubes. Mainly compression and bending tests were conducted to study the material energy absorbing behavior. Figure 2.2 shows the behavior of the thin walled hollow tube due to compression and bending.

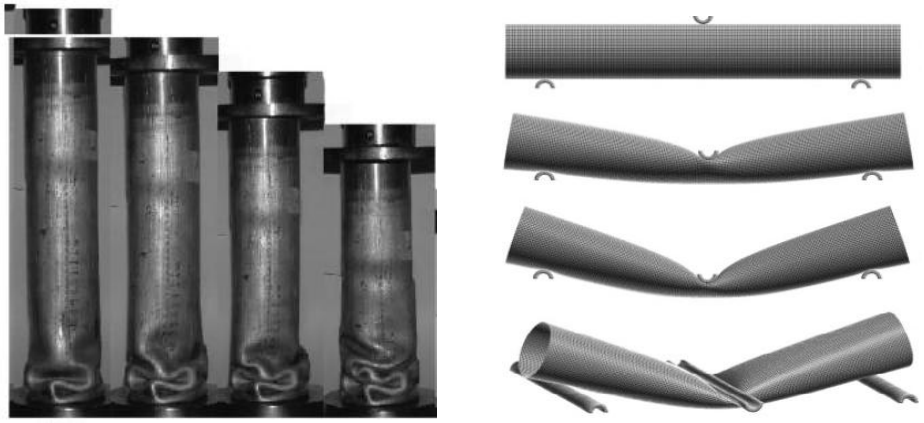

Figure 2.2 Behaviors of Cylindrical Tubes under Compression and Bending [1]

In both the cases, the energy absorption is observed as the tube undergoes deformation. In axial crushing or compression, the energy absorption is studied by the buckles or folds formed by the tube

collapse. In quasi static bending, the energy absorption is studied by Euler Buckling or bending deformation of the tube and the force required for bending. In general the deformation of a tube depends on the length (l), thickness (t), width (c) of the tube cross section. If this buckling behavior can be controlled, large amount of energy can be absorbed during deformation of the tube. This ideology of controlling the buckling behavior of crashworthy helped researchers to direct their work towards introducing filler materials into these crashworthy tubes to control the buckling behavior to a progressive deformation, which in turn increase the stiffness, stability and energy absorption capacity of the tube.

2.2 Importance of Foam as an Energy Absorbing Material Inside a Vehicle

Researchers have been coming up with new innovative ideas and thoughts in order to reduce the injury to the occupants inside the vehicle during an accident or impact. One such idea is the application of structural foam in a vehicle. Foam materials for structural applications are gaining significant attention in the auto and aircraft industries due to their good mechanical properties and light weight to strength ratio. They are light weighted with low mass and possess good energy absorbing and insulation characteristics. The structural foams nowadays are being used in automobiles to improve the safety of occupants.

Engineers like Slik et al [10] conducted study on model validation of a high efficient energy absorbing foam for head and pelvic protection during an impact. According to FMVSS 201U, impact sled tests with rigid impactor shape dummy pelvis and head free motion head were conducted to validate the models and access the characteristics of the foam materials in protecting the head and pelvis. The impacts tests with pelvic shaped impactor is conducted on block, cone and pyramid shaped foams and the head impact tests is performed with a free motion head form. Both the head and pelvis blocks are impacted to the foam material and energy absorption characteristics are studied.

The head impactor model was modeled as shown in Figure 2.3. The steel block represents the body- in- white steel member with a foam pad attached to it. The head block is impacted at a certain speed to the steel profile with foam pad and without foam pad.

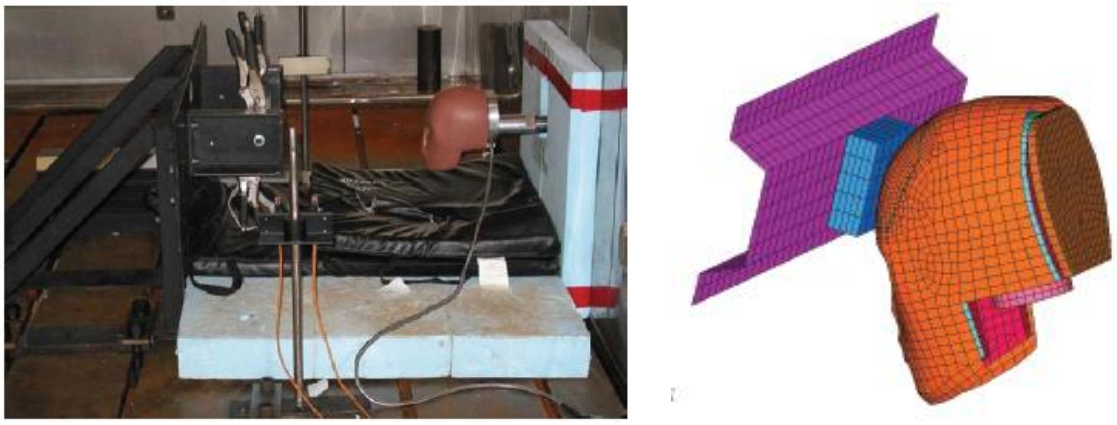

Figure 2.3 Head Impact Setup and FE Simulation [10]

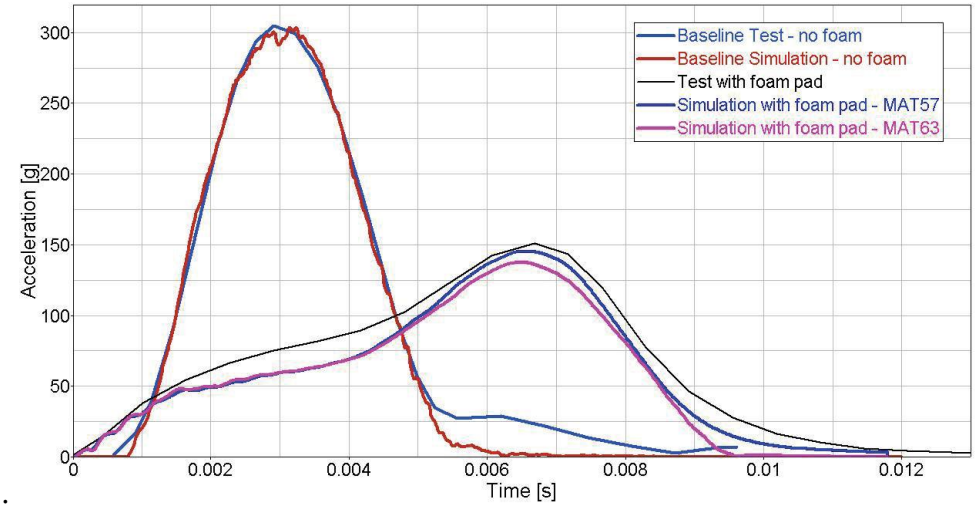

Figure 2.4 Acceleration vs Time for FMH Simulation and Test [10]

The accelerations were measured at different time interval for both the cases. It can be clearly observed that the test and simulation with foam pad impacts shows the reduction in accelerations compared to that of no foam pad from Figure 2.4.

Similarly, the pelvic test set up was modeled as shown in Figure 2.5. The pelvic impactor hits the steel profile with and without foam pad at certain speed. The energy absorbing characteristics were studied using Force vs Displacement curve. The foam pad exhibits more energy absorption characteristics compared to without foam pad as shown in Figure 2.6.

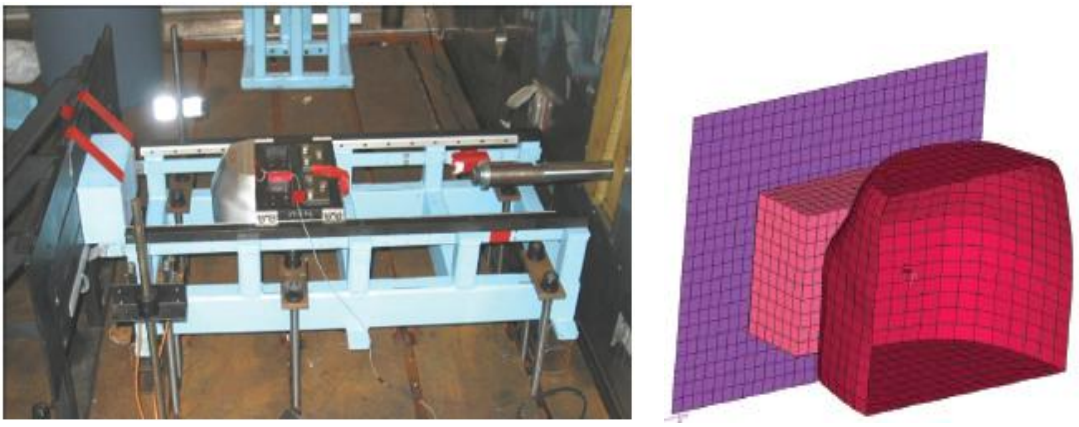

Figure 2.5 Pelvic Impact Setup and FE Simulation [10]

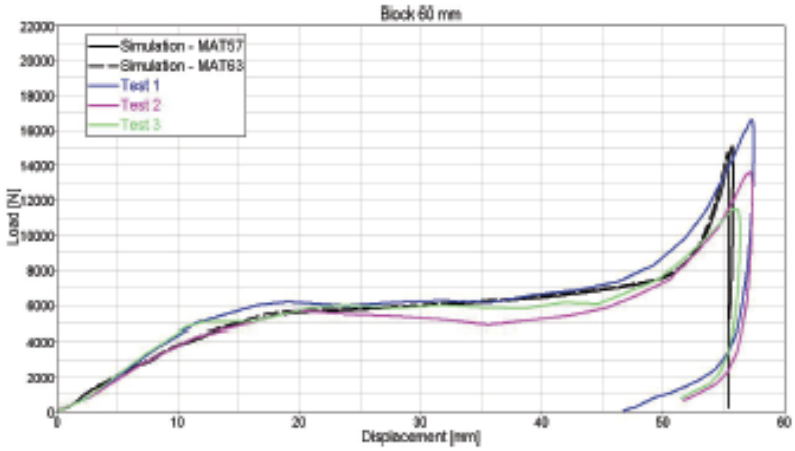

Figure 2.6 Load vs Displacement with Foam pad [10]

The study concludes that the foam pads possess high energy absorbing characteristics and can be utilized for protection of occupants during an impact.

2.3 Characteristics of Foam as Energy- Absorbing Material

Foam is defined as a substance which is formed due to the entrapment of pockets of gas in liquid or solid. It is extremely composite systems with poly disperse gas bubbles separated by draining films [7]. Foam can be created using endothermic (heat) or exothermic (mixing of chemicals) process. There are different types of foams such as solid foams, liquid foams, syntactic foams and integral skin foams used for different applications depending on the nature of their behavior. Foams are nowadays widely used in almost every industry due to their good thermal and mechanical properties.

Foams that are used in automotive industry for structural applications are mostly solid foams which are porous in nature. Different types of metallic and nonmetallic foams characterized by their mechanical properties are being used for several applications in an automobile such as acoustic insulation, window seals, structural stiffness, light weight body panels, seat cushions, vibration dampening and energy absorbers in crashworthy structures like bumpers, rails, pillars etc. As energy absorption plays a major role in crashworthiness, the energy absorbing foams in structural applications got more attention in the automotive industry.

2.3.1 Solid foam materials

Foam materials are characterized based on their application and mechanical behavior. In engineering applications especially automotive, solid foams which are lightweight materials (metallic or plastics) are being used. Solid foams are distinguished into two types namely open cell and closed cell foams. They are generally characterized based on the core structure of the foam material as shown in Figure 2.7.

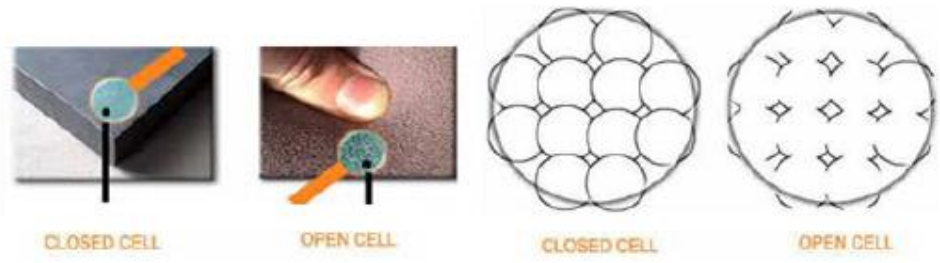

Figure 2.7 Closed cell and Open cell Structure of Foam Material [17]

Open cell foam: Open cell structured foams are relatively soft and less dense as shown in Figure 2.8. They have interconnected pores forming a network linked to each other. Open cell foams are more permeable to moisture vapor which gives space to air or liquid to fill in the pores making the foam soft and weak. Open cell foam can often be used as a good insulator and as an effective sound barrier. They are porous having a soft spongier appearance, with low strength and rigidity compared to closed cell structured foams. Figure 2.8 shows the physical and cell structured open cell foam.

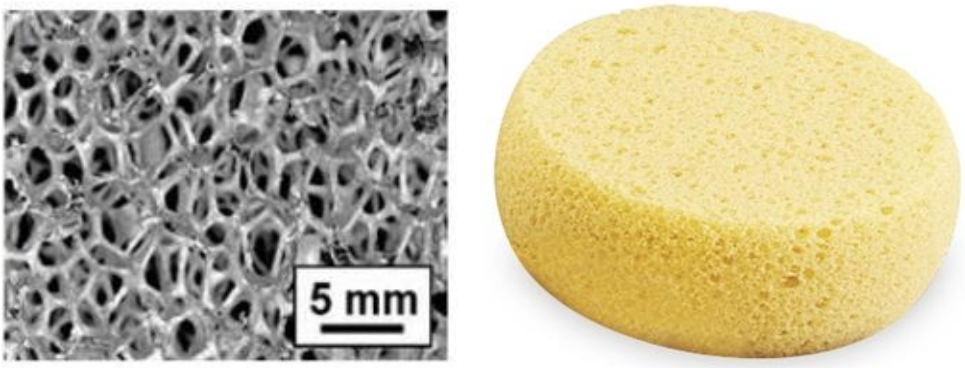

Figure 2.8 Open Cell Structure of Foam Material [17]

Closed cell foam: Closed cell structured foams are relatively dense and stiff as shown Figure 2.9. They do not have interconnected pores and due to their core structure with pores close to each other, these foams tend to have high compressive strength. Closed cell foams are often characterized by their high strength and rigidity. Compared to open cell structured foams, these foams have low moisture vapor permeability and high dimensional stability. These foams are often used as good insulation in vibration applications due to the entrapment of air in the closed cells. The wide range of industrial applications of these closed cell foams include shock absorbers, energy absorbers, insulation, vibration dampening, cushioning products and packaging etc. Due to their high thermal and mechanical properties and high compression strength, they are nowadays widely used in automotive and aerospace industries in structural applications.

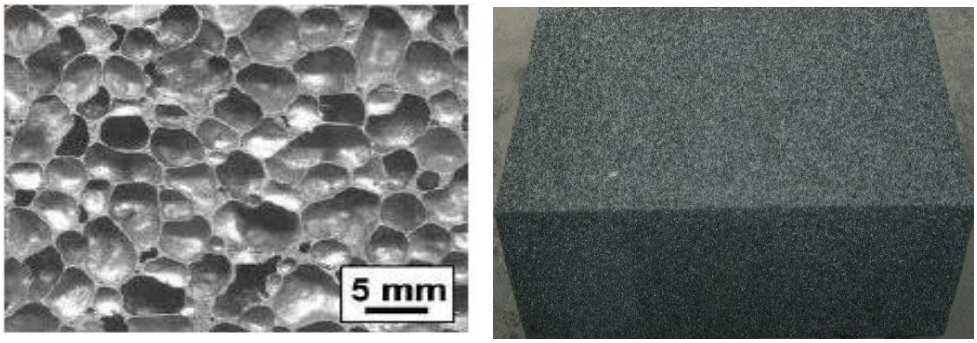

Figure 2.9 Closed Cell Structure of Foam Material [17]

In automotive applications, these closed cell foams are used in vehicle interiors like seat cushions, padded material in door panels, insulation, in the car headliners etc. Since the closed cell foams are rigid

with high compressive strength, they are often used as energy absorbers in crashworthy structural elements of the vehicle. Great amount of time and research is being carried over in this direction. Researchers developed various foams with good energy absorbing and compression strength properties. One such foam which has gained attention in the automotive industry is the polyurethane foam. It is being used as a widespread impact material for safety in automobiles.

2.3.2 Reinforcement of crashworthy tubes with foam filling

It is a proven fact in automobile industry that reinforcement of crashworthy tubes not only increases the optimal performance of the vehicle under various load cases during a crash, but also increases the structural integrity of the vehicle. Several approaches are available to control energy during a crash and also alter the crash signature, such as fabrication of steel for improved structural strength, engineered thermoplastics and polymer foams. The crash performance of the vehicle also needs to align with the light weight criteria due to the increase in demand for new materials and joining technologies in auto industry due to which the filler materials are considered as a good source in improving the crashworthiness of a structure with low mass addition and easy installation.

Studies and researches in this field showed that the axial crushing behavior of thin walled tubes is effective source to study the energy absorption characteristics but a study on the real world crash results presented by Kallina et al [14] in 1994 showed that up to 90% of crashes involved the structural members of the vehicle which failed in bending collapse mode. In general, for an empty thin walled column as it undergoes structural bending, it's bending resistance declines significantly after the reaching the peak force. In order to achieve the high bending resistance and weight efficiency in energy absorption, foam materials are introduced into the thin walled empty structures [11]. Many researchers spent enormous amount of time and resources to study the effect the foam filling into these crashworthy tubes. Metallic foams has gained significant attention in recent years, as they have good energy absorbing characteristics and also acts as shielding devices to reduce the shock waves due to the deformation forces. Metallic foams usually are made of Aluminum, titanium, platinum, Iron, nickel and copper.

Aluminum and polyurethane foams are often termed as the famous foams because of their light weight, low density and high energy absorbing capacity. Great amount of time and research is being carried on these foams to study and improve their energy absorbing characteristics. Researchers like Shigeaki et al [15] conducted studies on the aluminum foam to characterize its energy absorbing behavior under quasi static bending condition. Figure 2.10 shows three- point bending test of Aluminum foam filled steel tube.

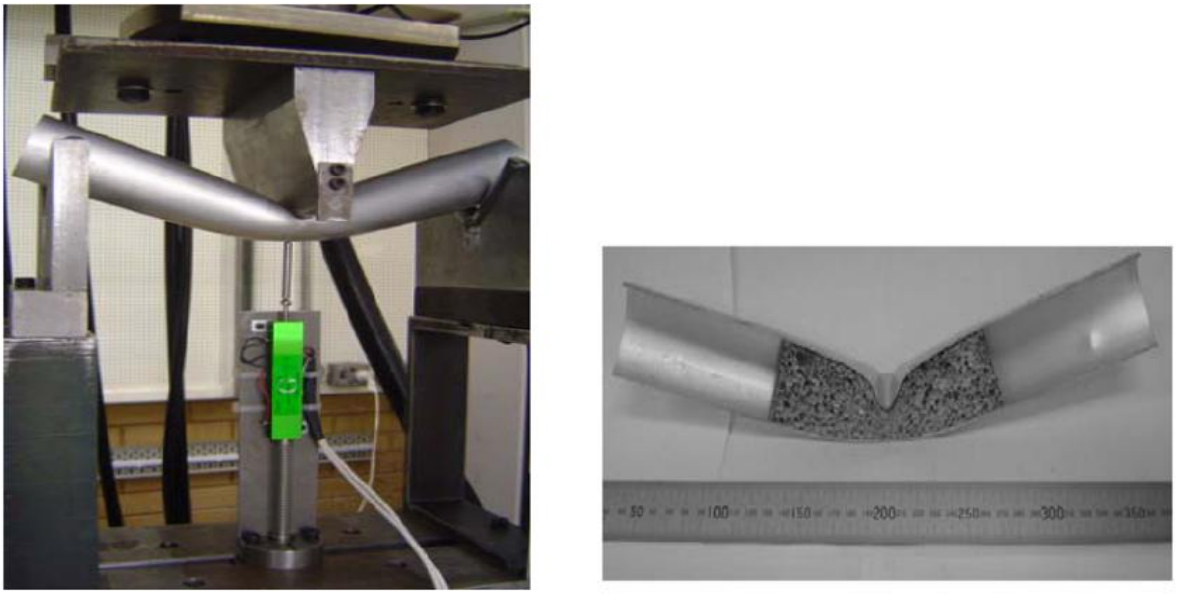

Figure 2.10 Foam Filled Tube under Bending [15]

The load displacement characteristics' of the tube with and without the foam were studied. The lowest generator displacement with relation to Indenter movement is also observed. It is clearly shown in Figure 2.11, that the energy absorption of foam filled tube is higher compared to the empty tube.

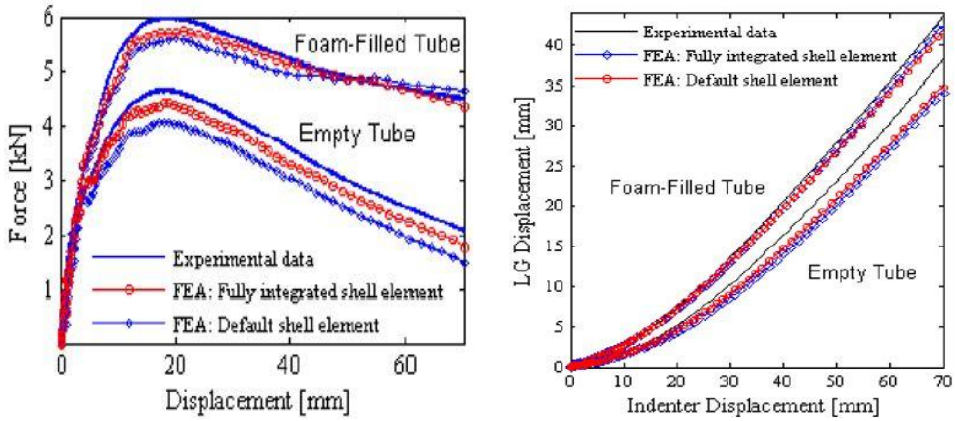

Figure 2.11 Load vs Displacement Characteristics of Empty tube and Foam Filled Tube [15]

In a study conducted by Droste, et al [16] on increase in crash performance with structural BETAFoam which is a mixture of two component polyurethane foam systems, it was found that the energy absorption of the tube with the BETAFoam is doubled compared to the hollow tube when a three point bending test was performed as shown in Figures 2.12 and 2.13.

Figure 2.12 Bending of Hollow Tube and Tube Filled with BETAFOAM [16]

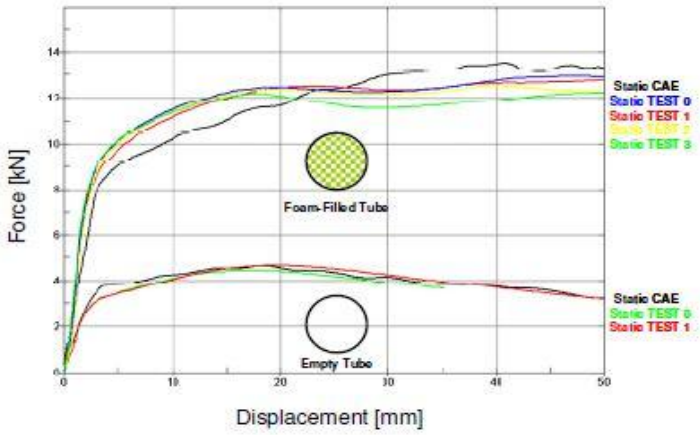

Figure 2.13 Force vs Displacement of Empty tube and Foam Filled tube [16]

2.3.4 Mechanical properties of foam materials

Foam materials are often characterized by their mechanical properties. These mechanical properties help researchers to classify the behavior of the foam material. Even though these foams possess good thermal and mechanical properties they are affected by adding the fillers or base material. The important mechanical properties to be considered to classify a foam material are foam density, foam modulus and crush strength.

- **Density of foam**

The actual foam density (ρ_A) can be calculated by multiplying the bulk density (ρ_B) as of the base material of struts or ligaments to the Relative density (ρ_R) [17]. It can be shown as:

*Actual density = Bulk density of base material * Relative density of foam*

$$\rho_A = \rho_B - \rho_R \tag{2.1}$$

In general, the ranges for typical foam relative densities are 2% to15% for metal foams, 3% to 4% for carbon foams and 3% to 20% for ceramic foams.

Another simple way to determine the density of foam is to measure the weight of the foam (100% solid material) and divide the measured weight by the calculated weight.

- **Elastic modulus of foam**

The foam modulus is a function of elastic modulus of solid material and square of the foam structure relative density. This can be defined by equation 2.2 [17].

Modulus of foam = Modulus of solid * Relative density ^{2}

$$E_f = E_{s.}\,(\rho_r)^2 \tag{2.2}$$

Where, E_f is the modulus of elasticity of the foam material, E_f is modulus of elasticity of the base material or strut and ρ_r is % Relative density of the foam

- **Crush strength or plastic yield strength**

After foam modulus, the most frequently considered mechanical property is the crush strength or the plastic yield strength of the foam. According to the young's modulus equation, the foam initially

yields when the load is applied to the foam structure. However, based on the foam size and at approximately 4% to 6% of strain, the foam beings to buckle and collapse at a constant stress continuously. Based on the initial relative density of the foam, this constant collapse occupies 50-60% of strain. At this point, the stress/ strain rises as this compressed foam enter into the densification phase. Crush strength of the foam is defined as the point where stress/ strain curve transition from elastic phase to plastic deformation phase. It is a very important mechanical parameter as it should remain below the crush strength phase for any structure to maintain its shape and under the design load.

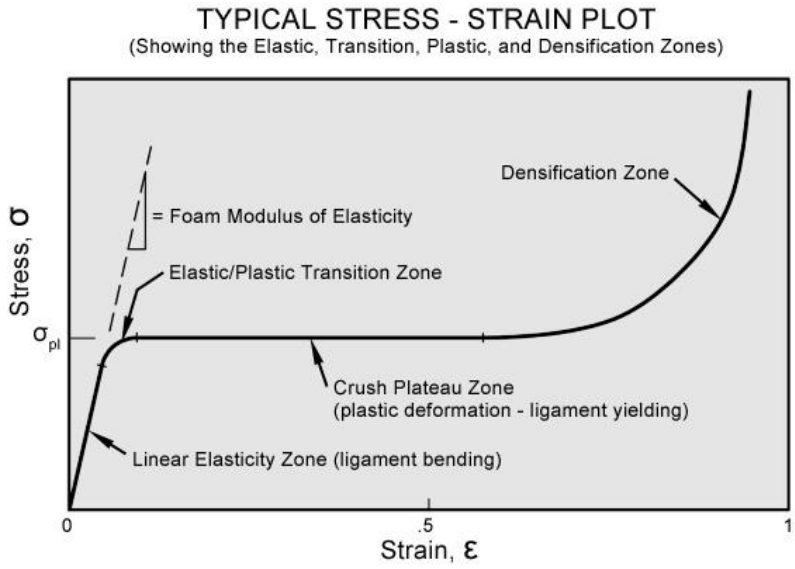

Figure 2.14 Typical Stress vs Strain Curve [17]

As shown in Figure 2.14, the work defined as force times displacement is the flat section of the curve between the 4% to 6% transition and 50 -70% of constant collapse. This exclusive characteristic of these porous materials makes them good energy absorbers. Here, the kinetic energy of the mass impacted is absorbed in parallel to the controlled loads. For both rigid and collapsible foam structures, crush strength (σ_c) is an important design characteristic. It can be shown as [17]:

$$\sigma_{cs} = 0.58 \times \sigma_{\gamma r} \times (\rho_r)^{3/2} \tag{2.3}$$

Where, σ_{cs} is Crush strength of the foam material, σ_{ys} is tensile yield stress of foam struts, ρ_r is Relative density of foam

The other important parameters to take into consideration when looking at foam properties are its foam material, pore size and relative density which are the independent variables. It makes the characteristics of foam as functions of any of these independent variables.

2.3.5 Effect of nanoparticles on foam properties

Nanotechnology is considered as one of the promising approach in material sciences. Introducing fillers or doping has become a common approach in changing the material properties of any material. Scientists are continuously developing composite materials for improved properties of the material for different applications in this field. One such composite material in automotive industries which gained significance in recent years is the composite foams. These foams are usually in the form of a sandwich having face sheet materials on both side and a core in the middle. The face sheet materials are usually strong and stiff and carry most of the structural load, whereas the core inside is usually weak. Improving the thermal and mechanical characteristics of the core can increase the bending stiffness and energy absorption capacity of the sandwich [18]. It also acts a good source of damping for the core as stress waves caused due to the impact loading propagates inside the sandwich material. Research has been carried in this field of introducing nanoparticles in the foam materials to improve their material characteristics. Nanoparticles typically range from 1 – 100nm possessing very high mechanical and thermal properties compared to that of polymers.

Researchers like Saha et al [18] worked on improving the material properties of these foam materials by infusing nanoparticles. They infused different nanoparticles into polyurethane foam and studied the mechanical characteristics of the foam. Three different types of nanoparticles namely spherical TiO2, nanoclay and rod-shaped carbon nanofibers (CNF's) were used and tested. In his study 1% of nanoparticles were added to the polyurethane foam. The results have shown significant enhancement in thermal and mechanical properties of the polyurethane foam as shown in Figure 2.15.

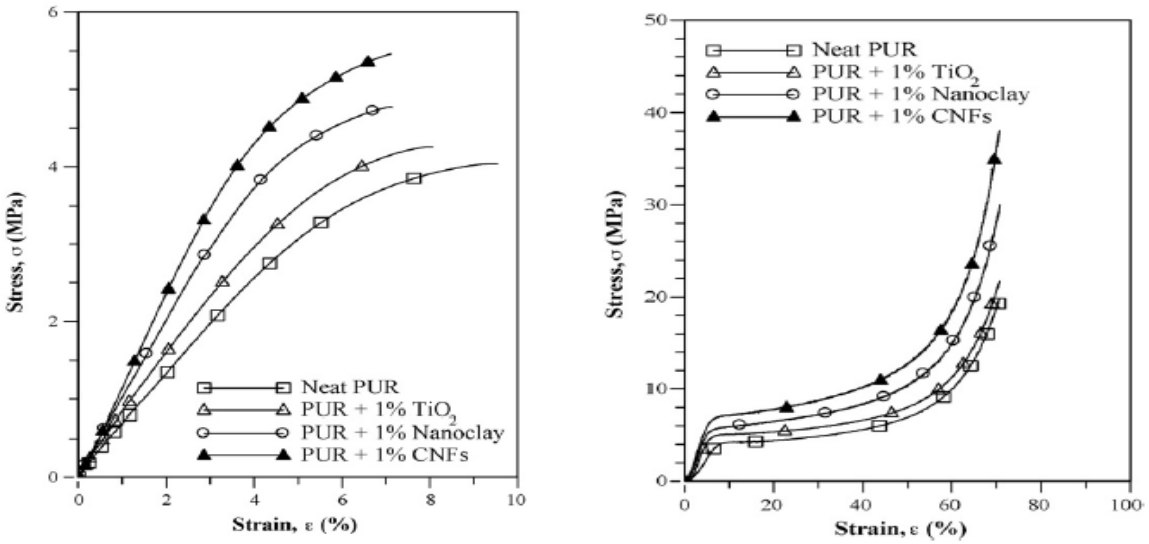

Figure 2.15 Stress vs Strain Characteristics of Different Foams during Tension and Compression [18]

Table 2.1 shows the compression test results of polyurethane foam after infusion of nanoparticles. Test samples are tested under compression until it reached 70% of densification. The results show that polyurethane foam infused with carbon nano tube particles shows better material properties than other nanofoams. There has been a significant amount of increase in the compression modulus and compressive strength of the polyurethane foam compared to other foams.

Table 2.1 Test results of different foam materials under compression [18]

Material	Sample No.	Compressive Modulus (Mpa)			Compressive Strength (Mpa)		
		Data	Average +/- SD	Gain (%)	Data	Average +/- SD	Gain (%)
Neat	1	133.6	130.2 5.4	-	4	3.7 0.3	-
	2	124			3.3		
	3	133			3.8		
1 wt% TiO2	1	137.9	146.3 7.3	12.4	4.1	4.3 0.2	16.2
	2	151.3			4.5		
	3	149.7			4.3		
1 wt% Nano Clay	1	164.8	156.7 7.2	20.4	5.1	5.1 0.1	37.8
	2	154			5.2		
	3	151.3			5.2		
1 wt % CNFs	1	180.5	182.4 2.3	40.1	5.8	5.8 0.1	56.8
	2	181.8			5.8		
	3	184.9			5.7		

CHAPTER 3

METHODOLOGY

3.1 Introduction

Foams are nowadays widely used for crashworthy structural applications especially in auto industry. Several engineers and researchers around the globe are working on improving the structural characteristics and its efficiency to withstand extreme impact conditions. As discussed earlier, foams are used in bumpers, railings etc. to improve the energy absorption capacity or increase the crush time during an impact or accident. One such application was studied by Droste, et al [16] using structural BETAFoam, where the increase in structural performance was observed by introduced the BETAFoam into the front rail and Roof rail of a Geo Metro and performed a full vehicle frontal crash analysis. It was clearly observed that the application of BETAFoam reduced the structural deformation significantly. The application of BETAFoam and the frontal crash simulations of the baseline and vehicle treated with BETAFoam is the Figure 3.1 and Figure 3.2.

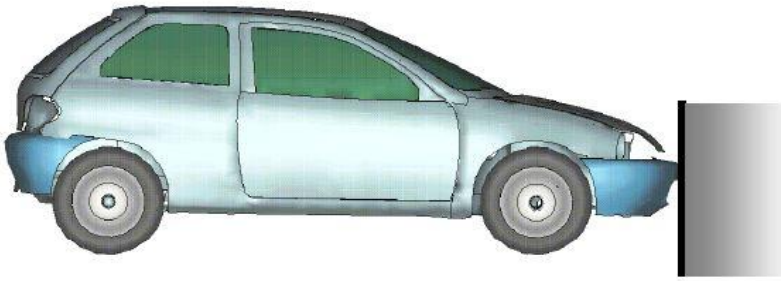

Figure 3.1 Geo Metro NCAC Model in Generic Frontal Crash Analysis [16]

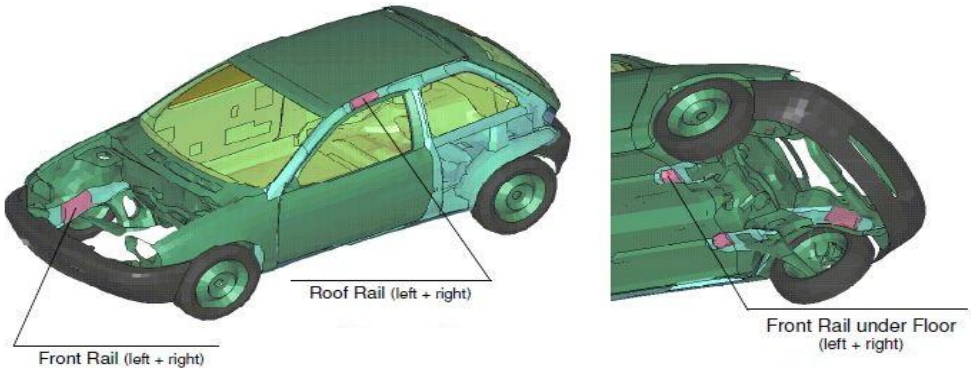

Figure 3.2 Structural Foam Applications in Geo Metro [16]

The structural deformation during the impact was observed. The deformation of the total car without foam was 736mm and 640mm with the foam treated car. Regarding the front end structure, the deformation of the original car was 578mm and 470mm with the foam treated car. The deformation pattern and results of the performance increase using the structural foam is shown in Figures 3.3 and 3.4.

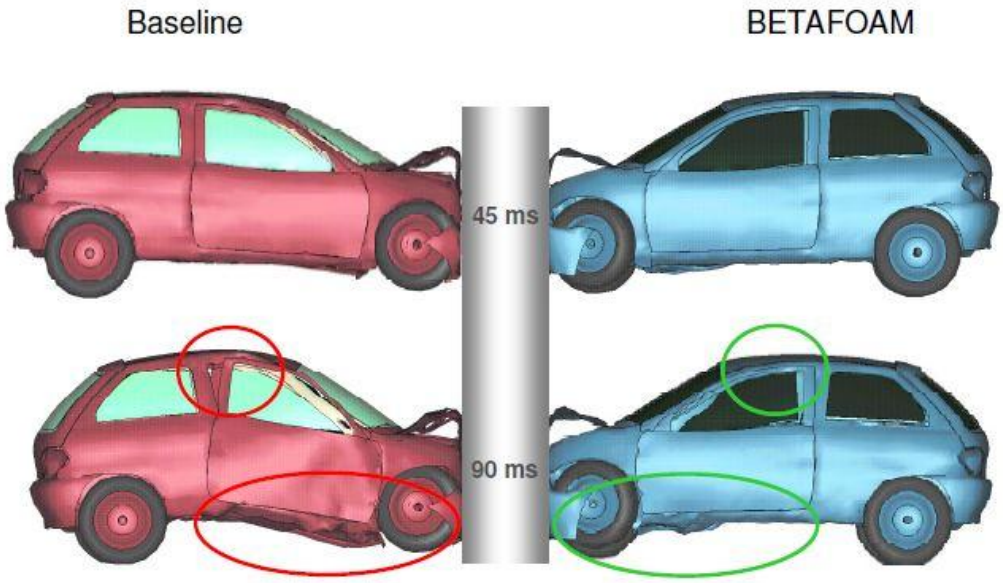

Figure 3.3 Baseline and Foamed Car Deformation in Frontal Crash [16]

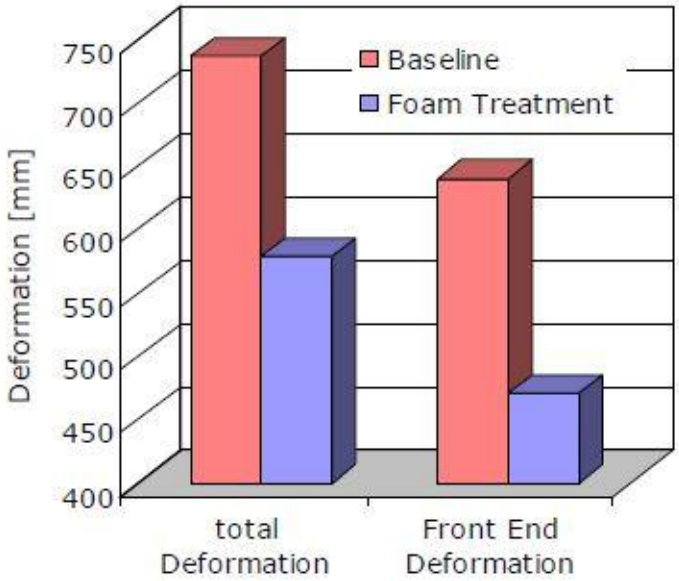

Figure 3.4 Deformation Results of Performance Increase using BETAFOAM [16]

3.2 Outline of General Methodology

Figure 3.5 illustrates the general methodology for this study. The detailed description of each step in the methodology is provided in the next sub sections.

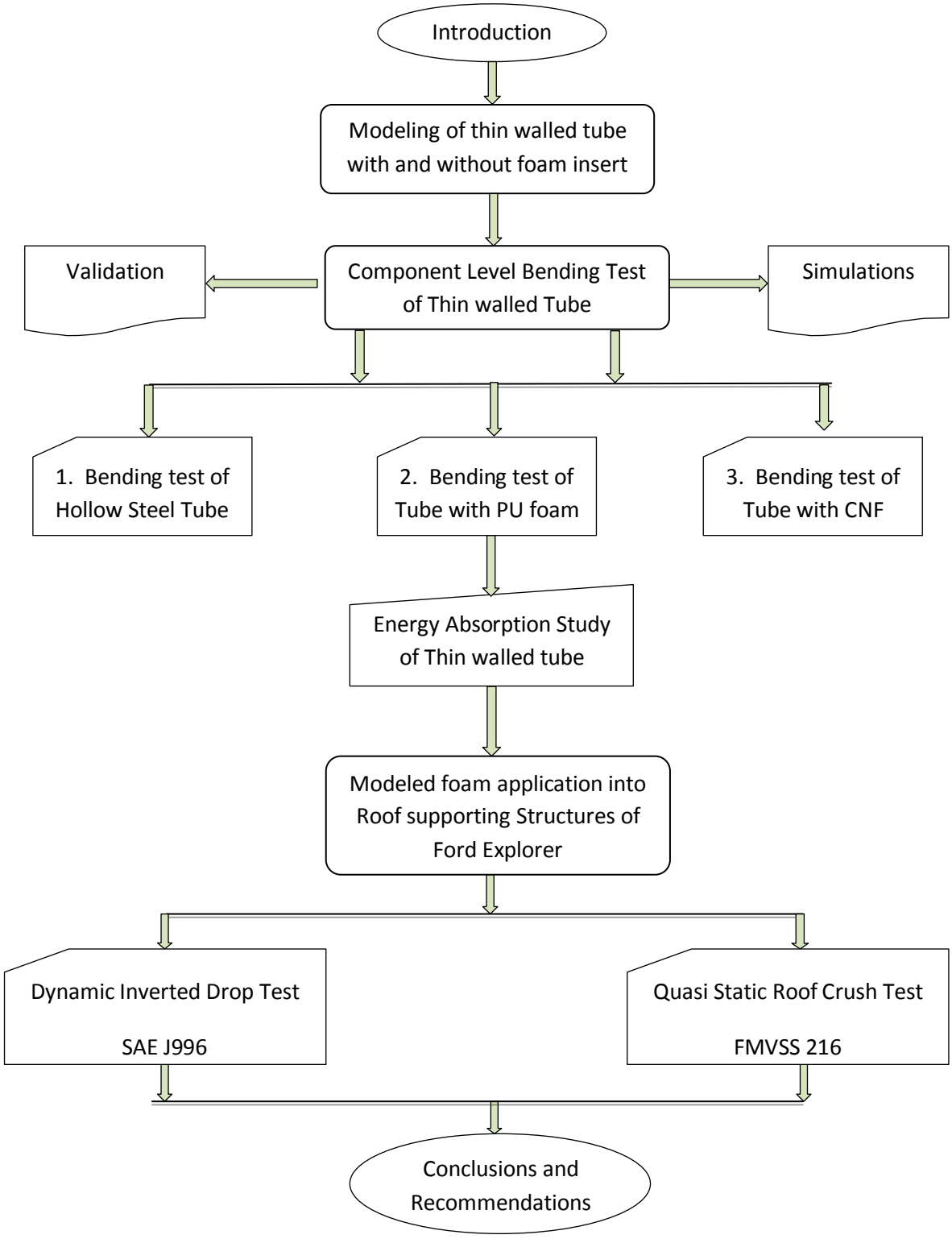

Figure 3.5 General Methodology of the Study

3.3 Component level Bending Test

The first phase of this study is to determine the energy absorption characteristics of the nanofoam. In order to characterize the energy absorbing capacity of the foam, a component level three point bending test will be performed on a steel tube with and without foam inserts. As shown in Figure 3.5, several steps are involved in this phase:

- A thin walled hollow steel tube is modeled for component level testing and a three point bending test is performed.
- The numerical results of the steel tube shall be compared with the experimental results to validate the model.
- The foam shall then be modeled and inserted into the hollow tube and the component level three point bending test simulation is performed on the steel tube for 3 different cases i.e, without any foam material, with polyurethane foam and with nanofoam.
- The simulations and results at all three conditions are to be observed and plotted.
- The energy absorption characteristics of the tube with and without foam materials shall be determined by force vs displacement curve.

3.4 Rollover Test for Determining Roof Strength

The second phase of the study is to determine the roof strength characteristics of a Sport Utility Vehicle (SUV) with and without foam insertion. As shown in Figure 3.5, the steps involved in the rollover testing phase:

- The foam will be modeled and inserted according to design of hollow roof supporting structures.
- Two different roof crush testing ie, static and dynamic testing will be performed on the vehicle to determine the roof strength characteristics at both the events.
- A quasi static roof crush simulation and inverted drop test simulations shall be performed and the energy absorption characteristics without with foam insertions are observed and quantified. Details of both of the tests are provided next.

3.4.1 NHTSA Standard testing procedures

The National Highway and Traffic security Administration (NHTSA) is dedicated to achieve high standards of excellence in motor vehicle and highway safety. Due to the increase in concern of safety in cars, public pressure grew in US in late 60's, which led to the implementation of safety regulations and guidelines in all the motor vehicles. NHTSA was officially established to administrate and ensure the safety and protection of the occupants inside the vehicle by conducting various tests, implementing guidelines and regulations on vehicle design, manufacturing and safety performance.

Rollover accidents have become one of the most important concerns for the safety of vehicle occupants. Due to the increasing concerns of higher fatality rates, NHTSA implemented different standards for the auto makers to regulate the roof crush in incident of a rollover. Various other organizations like Society for Automotive Engineers (SAE) and Insurance institute for Highway Safety (IIHS) also contribute in making guidelines for standards and test procedures. There are different testing procedures and guidelines for a vehicle to regulate the roof crush during a rollover scenario, in which SAE J996 (Dynamic invert drop test) and FMVSS 216 (Static roof crush testing) gained much importance, as they depict the actual roof crush during a rollover scenario.

3.4.1.1 SAE J996: Dynamic Invert Drop Test

SAE J996 was developed by society of Automotive engineers (SAE) in late 1960's and is considered to be one of the promising test to study the roof crush deformation in a rollover scenario. There are different advantages endorsing invert drop test as following [21].

- The lateral or slip velocity between the pavement and the vehicle is considered, this shows the real dynamics of the roof crush and its geometry evaluating the injuries to occupants inside the passenger compartment of the vehicle.
- Both sides of the vehicle roof with the windshield impact are being tested and the harm caused to the occupant is more evident as the wind shield breaks and shatters after during the impact.

The SAE J996 standard requires that [5]:

- The vehicle is hanged or inverted upside down at a roll angle and pitch angle of 25^0 and 5^0 respectively.
- The vehicle is dropped from a certain heights and the suggested drop heights are generally 12 inches and 18 inches.
- The drop heights are also calculated by the energies associated with the quasi static roof crush. It can be represented as [21]:

$$DH = E_s \times (\frac{1}{W \times g}) \tag{3.1}$$

Where, DH is the drop height in (m), Es is Static roof crush energy in (Nm), W is mass of the vehicle in (kg), g is the acceleration due to gravity in (m/s^2)

The Dynamic Inverted drop test setup is shown in Figure 3.6.

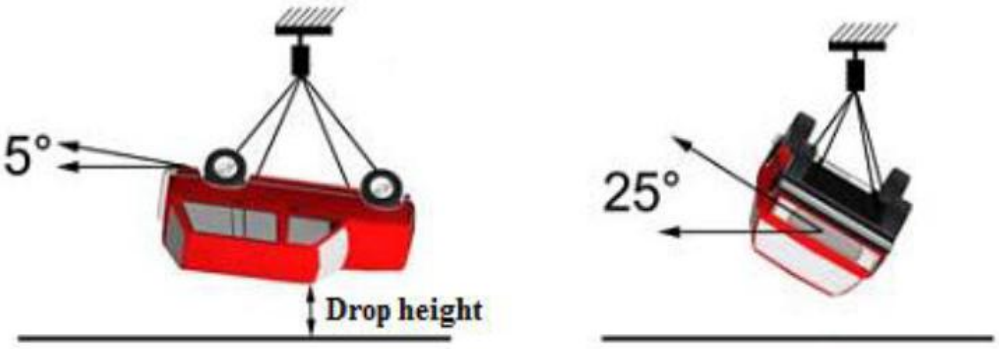

Figure 3.6 Dynamic Inverted Drop Test Setup [5]

3.4.1.2 FMVSS 216: Static roof crush test

Roof crush resistance due to vehicle roll over is an important concern in the automotive industry for the safety of public and occupants of the vehicle. The FMVSS 216 was first established in 1971 to decrease the roof collapse in an event of rollover. It is also known as quasi static roof crush testing establishing strength requirements for the passenger compartment of passenger cars, sport utility vehicles, multipurpose passenger vehicles with a GVWR of 6000 lbs or less [19]. The main intent is to minimize

the injuries to occupants and casualties in the event of rollover due to roof intrusion. Figure 3.7 shows the FMVSS 216 testing setup.

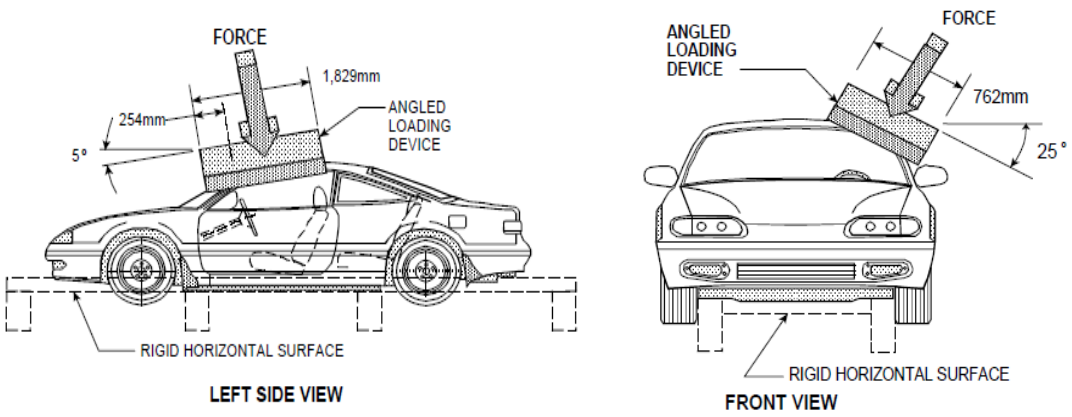

Figure 3.7 Quasi Static Roof Crush Test Setup [19]

The FMVSS standard requires that [19]:

- The vehicle is placed rigid and positioned on a horizontal surface with its doors locked and windows closed.
- The vehicle roof should withstand a load of 5000 lbs or 1.5 times the unloaded vehicle weight (UVW) multiplied by 9.8 or 22,240N (whichever comes first).
- The same standard is applied to passenger vehicles, cars and busses with gross vehicle weight rating (GVWR) of 6000 lbs or less.
- The load is applied using a rigid rectangular plate measuring 762mm wide and 1829mm long.
- The load or force is applied in downward direction at the front header with a speed not more than 13 millimeters per second until reaching the compliant resistive load.

The orientation of the rigid plate is equally important to the load applied and the direction of forces. The static loading device should be moved without any rotation, in a straight line with the lower surface of the plate is oriented as follows [19]:

- The plate's longitudinal axis is positioned or pitched 5^0 in forward direction below the horizontal from the side view as shown in Figure 3.2. Its lateral axis or the roll of the plate is at lateral outboard angle, 25^0 below the horizontal in the front view projection.

CHAPTER 4

FINITE ELEMENT MODELING AND VALIDATION

4.1 Introduction

The Finite element method is a powerful technique originally developed to solve complex problems of elasticity and structural mechanics using numerical solution. The FEM analysis process is very typical and a sequence of steps are involved in carrying out the process depending on FEM environment and model based simulation of the physical systems or numerical approach to mathematical problems[22]. This type of FEM approach is also distinguished as physical and Mathematical FEM.

4.1.1 The physical FEM

This methodology is also named as *model based simulation*. In this type of FEM process, the physical system acts as the center piece to be modeled due to which it is named as physical FEM. The process is well illustrated in Figure 4.1.

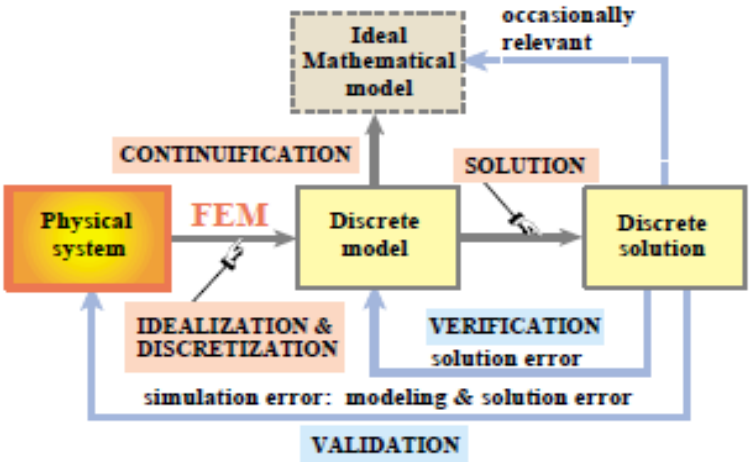

Figure 4.1 Physical FEM process [22]

The physical system is the point of concentration which is to be modeled. The idealization and the discretization processes which produce the discrete models are run parallel followed by the discrete solution or solutions attained by a -solution step handled by an equation solver. The ideal mathematical model often acts as a range limit or continuity of the discrete models. In a physical FEM the concept of error rises in two ways verification and validation. Here, verification can be done by replacing discrete

solution with the discrete models to get the solution error and Validation which is often termed as an important approach to determine the correlation of FE results compares the discrete solution against the observation or experiments computing the simulation error [22].

In general, the physical FEM discretization or idealizations can be shown and adjusted without the mathematical models, so that it can better represent this configuration. This method is also as model updating as shown in Figure 4.2.

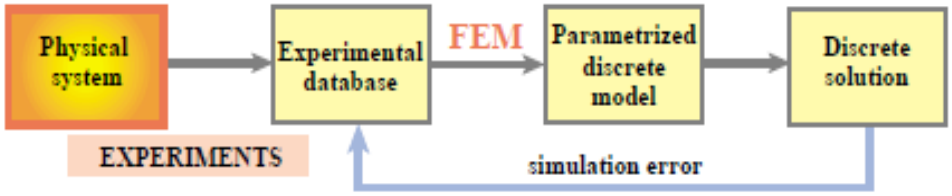

Figure 4.2 Model Updating process In the Physical FEM [22]

4.1.2 The Mathematical FEM

This way of FEM approach focuses on mathematics. In this process, the center piece of concentration is the mathematical model, which is often a differential or partial differential equation in space and time. In here, the FEM model is generated from a mathematical model and the FEM equations are solved as described in physical FEM [22]. The process is very similar to that of the physical FEM expect that ideal physical system is represented as realization of mathematical model and mathematical model is considered as the idealization of the system. This process is clearly shown in Figure 4.3.

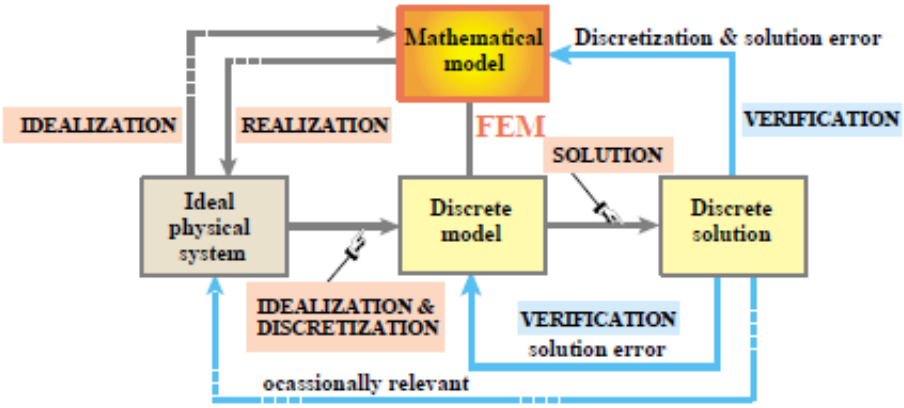

Figure 4.3 Mathematical FEM [22]

Understanding the synergy of physical and Mathematical FEM is very important when solving complex problems in automotive and aerospace fields. The Figure 4.4 shows the combination of physical and mathematical modeling through multilevel Finite element modeling.

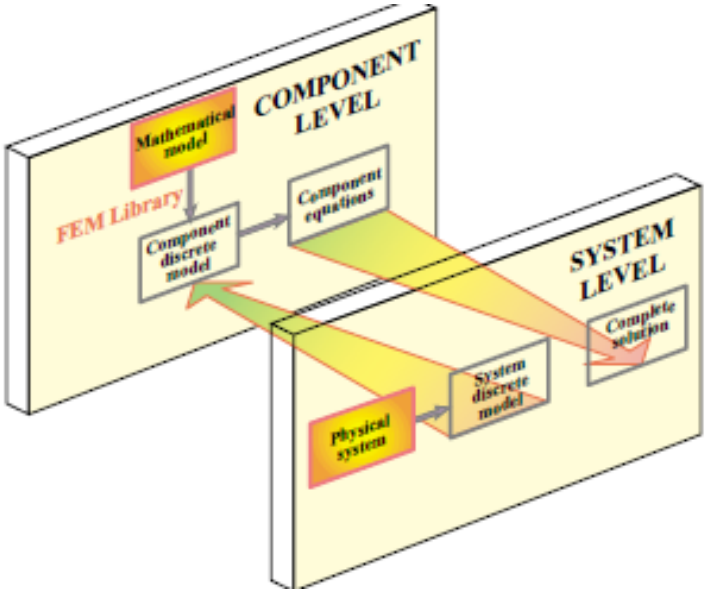

Figure 4.4 Combination of Physical and Mathematical Modeling through Multilevel FEM [22]

As shown in Figure 4.4, the various substructure of a final assembly are taken and broken down into several components. These components then become relatively simple in geometry which in turn can be well described in the mathematical models. The full system model is obtained by the process where, the component equations are transformed to substructure equations then to the final assembly. This assembly process is often governed by the principles of Newtonian mechanics.

4.2 Model Development and Validation

In the present study, a hollow steel tube undergoes a three point bending and is validated against the experimental results. This analysis case portrays the actual bending of the hollow roof structure of a vehicle during a rollover accident. Mamalis et al [1] has conducted a study on bending of thin walled cylindrical steel tubes and utilized explicit FE code LS- DYNA code to study the crush behavior and energy absorption characteristics of the specimen during bending.

4.2.1 Finite element modeling of tube structure

In the present study modeling of the thin walled hollow tube is carried using HYPERMESH and LS - Prepost. The model is modeled using all the boundary conditions. The explicit finite element code LS-DYNA is used to simulate the crush behavior of the hollow steel tube. The FE modeling of the hollow steel tube crushing process is carried in three steps. In the first step, the hollow steel tube is modeled using HYPERMESH and LS- Prepost. Secondly, the non linear dynamic analysis of the hollow tube crush is carried using LS- DYNA and finally the post processing of the hollow tube bending simulation results are interpreted and visualized using LS- Prepost.

4.2.2 Material and contact modeling

The steps involved in the simulation process and the parameters that are required to develop the finite element model are carefully done, to obtain an accurate and efficient FE model for the study. The FE model generation, contact interface between the parts, the various types and properties assigned to the model and the boundary conditions or constraints specified to the Finite element model are discussed as follows:

- The material used for the hollow steel tube is Low carbon steel with material properties as shown in table 4.1.

Table 4.1 Material properties of Steel

Mass Density	$\rho = 7.83\ g/cm^3$
Youngs Modulus	E= 207 Gpa
Yield Stress	Y = 210MPa
Poisson's Ratio	$\upsilon = 0.3$

- The dimensional parameters of the model including the cylindrical hollow steel tube, rigid supports and the Indenter are:

  Outside Diameter of the hollow tube D = 30.0 mm

The wall thickness of hollow tube t = 1.4mm

The axial length of the tube L = 200mm

The Radius of the Indenter and Rigid supports R = 5mm

- The span length '*l*' between the two rigid supports is 160mm, along which the tube was axially centered as shown in Figure 4.5.

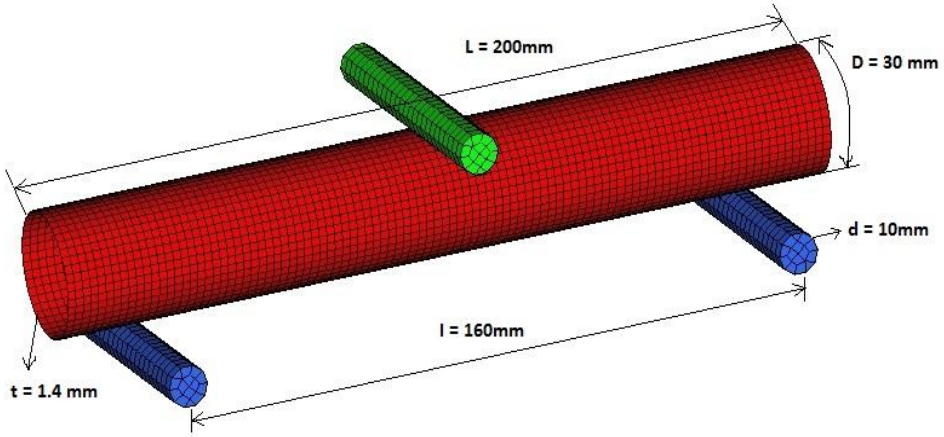

Figure 4.5 Dimensional Parameters of Three point Hollow tube Bending Setup

For finite element discretisation, the thin walled cylindrical tube is made up of low carbon steel and was modeled as an elasic- plastic material. MAT_24 (*MAT_PIECEWISE_LINEAR_PLASTIC) material card is used for the steel tube. Since this material card is based on linear isotropic plastic type, it utilizes von-mises flow rule. The tube was modeled using four node quad- shell element with 'Belytschko – Tsay' element formulation. This type of element formulations is used due to its high computational efficiency.

The Indenter and the two rigid supports have a circular cross section and are considered to be rigid members, modeled using eight node hexahedron solid elements. Material card MAT_20 (*MAT_RIGID) is used for the rigid members ie, the two rigid supports and the Indenter which are practically not deformed using the bend test. A constant stress solid element formulation is assigned to these rigid elements. A thickness of 1.4 mm is assigned to the hollow tube shell elements corresponding

to the actual model. The tube material is characterized by elastic plastic behavior with strain hardening and stress- strain characteristics as shown in Figure 4.6.

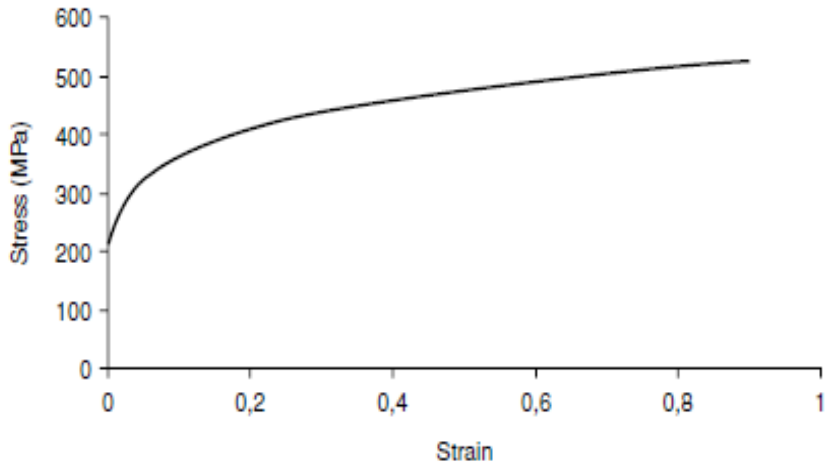

Figure 4.6 Stress vs. Strain Curve of Low Carbon Steel [1]

To specify the sliding interface between the hollow tube, rigid supports and Indenter, a *CONTACT_AUTOMATIC_SURFACE_TO_SURFACE contact card was selected considering all the boundary conditions. This sliding contact interface is a penalty formulation in which the 'slave' contacting segment is assigned to the hollow tube and the master contacting segment is assigned to the rigid supports and the Indenter. Table 4.2 shows the FE model details of the hollow tube.

Table 4.2 FE Model details of Hollow Steel Tube

Element length of tube model	2mm
Number of nodes in tube model	5641
Number of elements in tube model	5594

Kinematical boundary condition objectives are being specified to the Indenter which is a rigid body with five degree of freedom. The Indenter is moved with a constant velocity of 1m/sec in the vertical axis. This load was applied using *BOUNDARY_PRESCRIBED_MOTION_RIGID card. The velocity of the moving Indenter was high due to the explicit nature of the FEM code and not due to the specimen collapse under high strain rate loading [1].

4.2.3 Failure criteria

Generally tubes are modeled using shell elements based upon their thickness. In the present analysis, the thin walled hollow steel tube is modeled with a thickness of 1.4mm using 4 noded quadrilateral shell elements. The 4 node quad shell elements with five through the thickness integration points depending on the Belytschko- Lin-Tsay element formulation helps in presenting macro scopic distortion in improved manner. This type of element formulation is used to improve the computational efficiency. Also, this particular model is based on assumptions such as co-rotational and velocity strain formulation simplifying the given mathematical equations. It also helps in avoiding complexities of non linear mechanics by embedding a co-ordinate system in the element and velocity strain [7].

4.2.4 Three point bending test simulation setup and Validation

The Indenter impacts the hollow tube with velocity of 1m/sec until the termination time equal to the diameter of the tube i.e. 30mm is reached. The experimental setup of three- point bending of the hollow circular steel tube was carried out in an INSTRON 4482 testing machine of 100kN loading capacity. The Figure 4.7 shows the Bending simulation of the hollow steel tube.

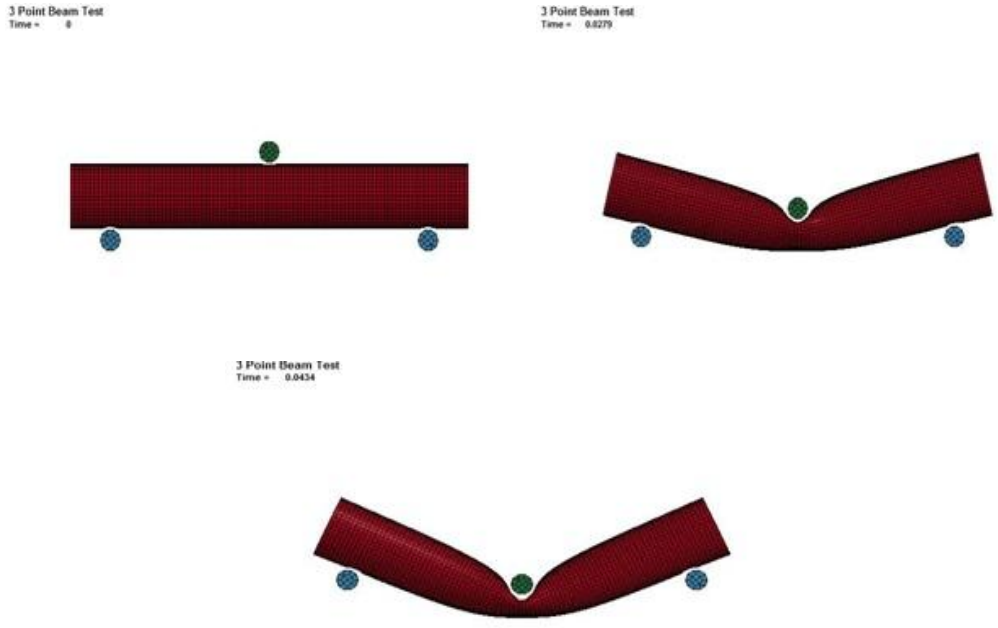

Figure 4.7 Three point Bending Simulation of hollow tube

The energy absorption characteristics of the circular hollow steel were compared both numerically and experimentally by a Load vs. Indenter displacement curve, as shown in Figure 4.8.

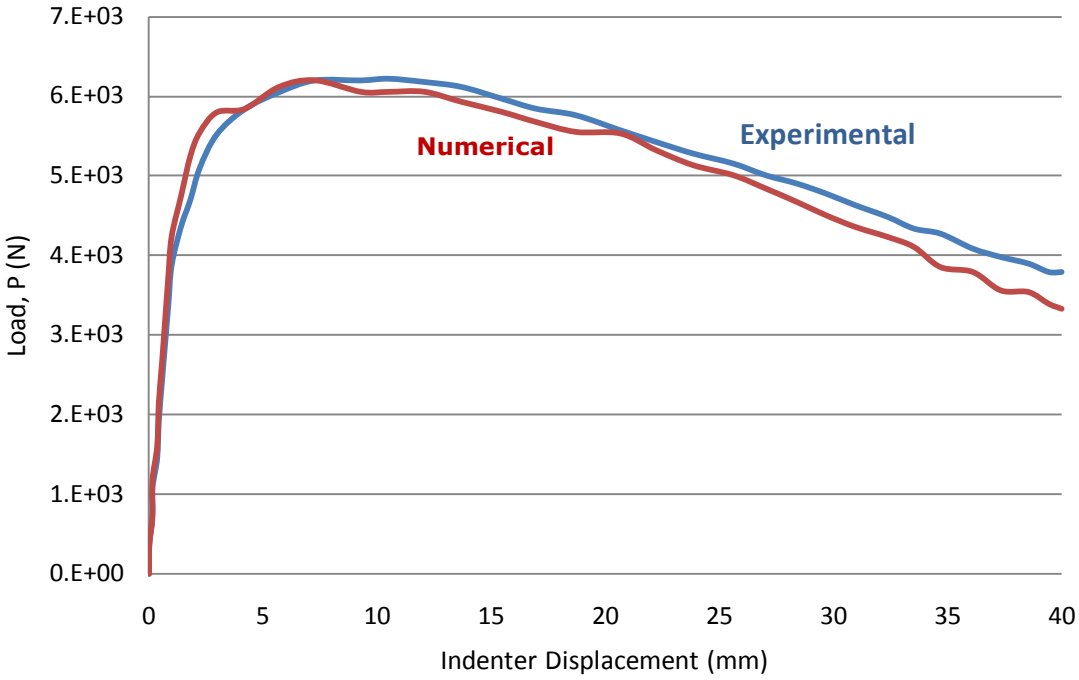

Figure 4.8 Load vs. Displacement Curve of Numerical and Experimental Bending of Hollow Tube

4.2.5 Results and discussion

As observed in Figure 4.8, the maximum peak load Pmax is 6.18kN at 12.4mm of Indenter displacement for the experimental, while the maximum peak load is 6.12kN at 8mm of Indenter displacement for the numerical simulation. The numerical deformation pattern was found to be in good agreement with the experimental pattern with 90% of correlation in area. Since the material model is validated and the energy absorption characteristics are similar to that of the experimental, the current model is used for further study of material properties and characteristics with different foam inserts.

4.3 Component Level Three point Bending Simulation with Foam Material and FE Analysis

The current thesis is based on studying the energy absorption characteristics of a vehicle roof with foam inserts in the hollow components of the roof supporting components. Accordingly, a hollow

cylindrical steel tube is validated which represents the roof crushing pattern during an impact scenario. Now, the hollow tube is filled with two different foams i.e, polyurethane foam and carbon nanofoam and then undergoes a similar three point bending test. The simulation comparison study at all three conditions gives an overview of the energy absorption and crushing behavior of the material.

4.3.1. Finite element modeling of cylindrical foam

The modeling of two foams i.e, Polyurethane foam and carbon nanofoam is the same but different material properties are assigned to both the foams. The FE modeling of the cylindrical foam is carried in HYPERMESH and LS- Prepost similar to the hollow tube modeling discussed in the earlier chapter. The foam is modeled to fit into the hollow tube and the analysis is done using the LS- DYNA code.

4.3.2 Material and contact modeling

Likewise discussed earlier, the material properties of thin walled hollow steel tube are the same, the steel tube modeled as an elasic- plastic material. MAT_24 (*MAT_PIECEWISE_LINEAR_PLASTIC) material card is used for the steel tube and the tube was modeled using four node quad- shell element with 'Belytschko – Tsay' element formulation. Material card MAT_20 (*MAT_RIGID) is used for the rigid members ie, the two rigid supports and the Indenter which are practically not deformed using the bend test.

The dimensions for modeling the foam are calculated based on the thickness and element size of the steel tube material. Generally, the element size of the foam materials is higher than that of the steel tube. The foam material is modeled with diameter (D) of 29.3mm, less than the diameter of hollow tube and with an axial length equal to the hollow tube i.e, 200mm as shown in Figure 4.9 and the FE model details of the foam are tabulated in Table 4.3.

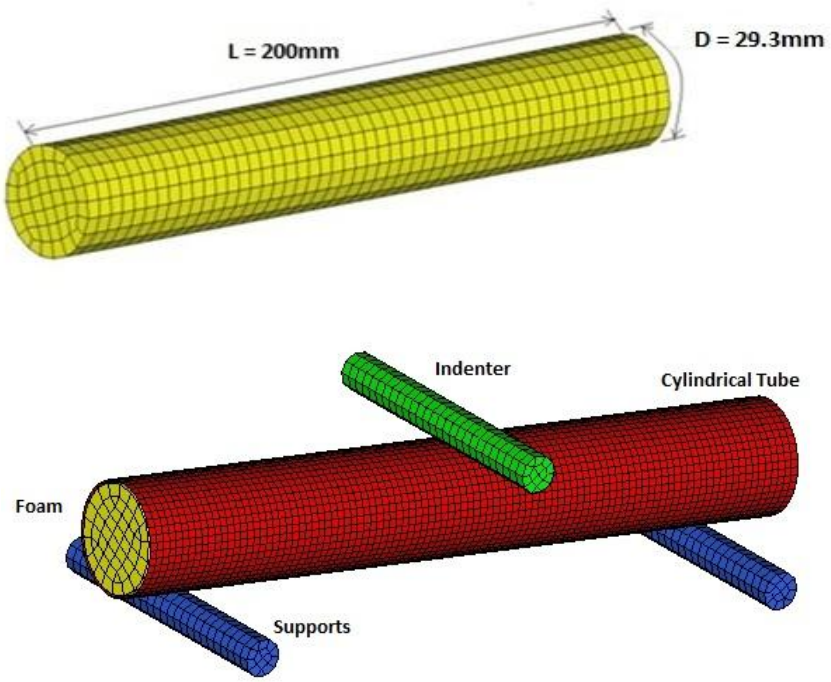

Figure 4.9 Dimensional Parameters of Foam Material and Three point Bending Setup

Table 4.3 FE details of Modeled Foam

Element length of foam	3mm
Number of nodes in foam	2856
Number of elements in foam	2250

The PU foam and CNFs are crushable with a very less recovery compared to the foams used in automotive and aircraft seating. There are different material models available for different types of foam materials. Generally, the common materials used for these type of foams are MAT_053 (*MAT_LOW_DENSITY_FOAM) and MAT_063 (*MAT_CRUSHABLE_FOAM) and *MAT_MODIFIED_CRUSHABLE_FOAM. Since the PU and CNFs are rigid foams, the strain hardening and strain rate effects are not considered. The MAT_063 i.e., *MAT_CRUSHABLE_FOAM material card is used for both the foam materials in the current model. The material properties of the PU and CNF foam are shown in table 4.4.

Table 4.4 Material properties of PU Foam and Carbon Nanofoam [18]

	CNF	PU
Mass Density	242.2 kg/m3	35kg/m3
Compression modulus	182.4 Mpa	135 Mpa
Compression strength	5.8 Mpa	3.7 Mpa
Tensile modulus	255 Mpa	137 Mpa
Poisson's Ratio	0.0	0.0
Tensile strength	4.4 Mpa	4.0 Mpa
Flexural modulus	207.3 Mpa	144 Mpa
Flexural strength	6.7 Mpa	4.8 Mpa

In the current model, the arbitrary yield stress and volumetric strain values are defined using a define curve. The volumetric strain is defined in terms of relative volume '*V*' [23]. It is shown as:

$$\gamma = 1 - V$$

Where, γ is volumetric strain and V is the Relative volume

Since, the lateral deformation is negligible, the poisson's ratio is considered to be zero and the volumetric strain is being replaced by linear strain. The stress vs. strain curve of both PU foam and CNF foam are shown in Figure 4.10, which are used as the load curves in the current model.

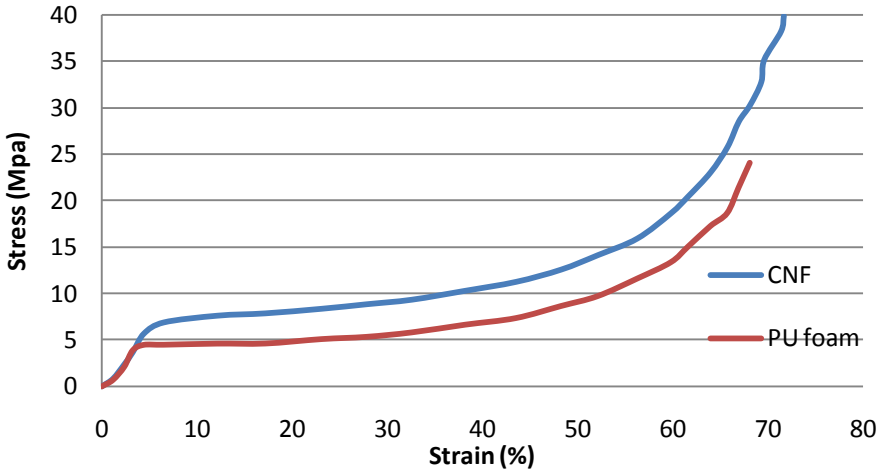

Figure 4.10 Compression Stress vs. Strain graph for PU Foam and CNF [18]

In a finite element analysis of any material models, one of the important concerns is assigning proper contact interfaces between different parts or components. The analysis output result depends on

these contact parameters. In this analysis there are 3 different contact interfaces defined between Rigid supports, hollow tube, foam and the Indenter.

A *CONTACT_AUTOMATIC_SURFACE_TO_SURFACE card is defined between the two rigid supports, hollow tube and the Indenter and a *CONTACT_TIED_NODES_TO_SURFACE is defined between the foam and the hollow tube. A constant stress element formulation is assigned to the foam material. A CONTROL_ENERGY card is assigned to the model where hourglass energy is computed and included in the energy balance. The sliding interface energy dissipation is not computed. The load for the model was applied using BOUNDARY_PRESCRIBED_MOTION card. A load of 1m/sec was assigned to the Indenter in the vertical direction.

4.4 Comparison of Hollow Tube with PU Foam and CNF Results

The component level bending simulation of the hollow tube with different foam insertions establishes a good example of the performance characteristics of foam materials. After introducing the foam into the hollow cylindrical steel tube, the necessary properties and boundary conditions are assigned to the model. The Indenter is moved with a high velocity in vertical direction impacting the tube. The energy absorption characteristics of the tube with PU foam and CNF are studied and conclusions are being drawn based on the results. Figure 4.11 shows the Load vs. Displacement results of tube bending.

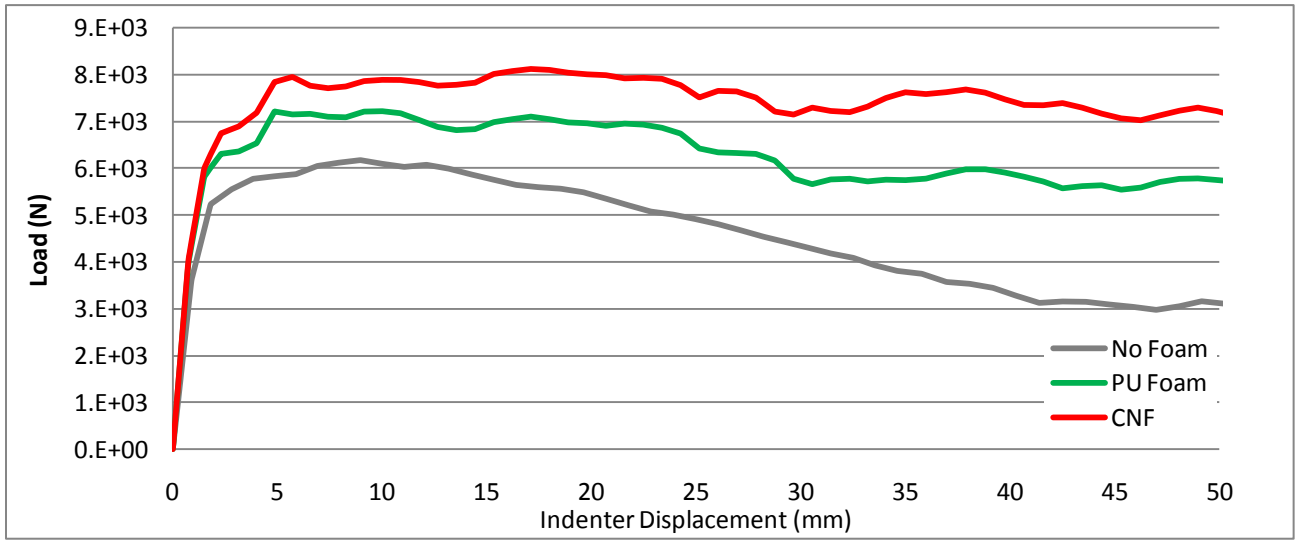

Figure 4.11 Energy Absorption characteristics of Tube with No Foam, with PU foam and with CNF

It can be clearly observed that, the peak loads vary for all the three conditions according to Figure 4.11. The peak load for low carbon steel tube is 6120 N and the peak loads of polyurethane foam and carbon nanofoam are 7220 N and 8120 N respectively. Also, the total energy absorbed by PU foam and CNF increased by 15% and 30%. Comparing all the three bending test results, carbon nanofoam exhibits more energy absorption than steel tube with polyurethane foam insert and hollow steel tube. The results are at three conditions are shown in table 4.5.

Table 4.5 Energy Absorption Characteristics of Tube Bending With and Without Foam Insert

	Peak load (N)	***% of Increase in Energy Absorption***
Hollow tube	6120 @ 8mm	Base
Hollow tube with PU foam	7220 @ 5mm	15%
Hollow tube with CNF	8120 @ 18mm	30%

The Bending test simulations of tube at 0.031sec for all three conditions i.e. with no foam, with PU foam and with Carbon nanofoam insert are shown in Figure 4.12.

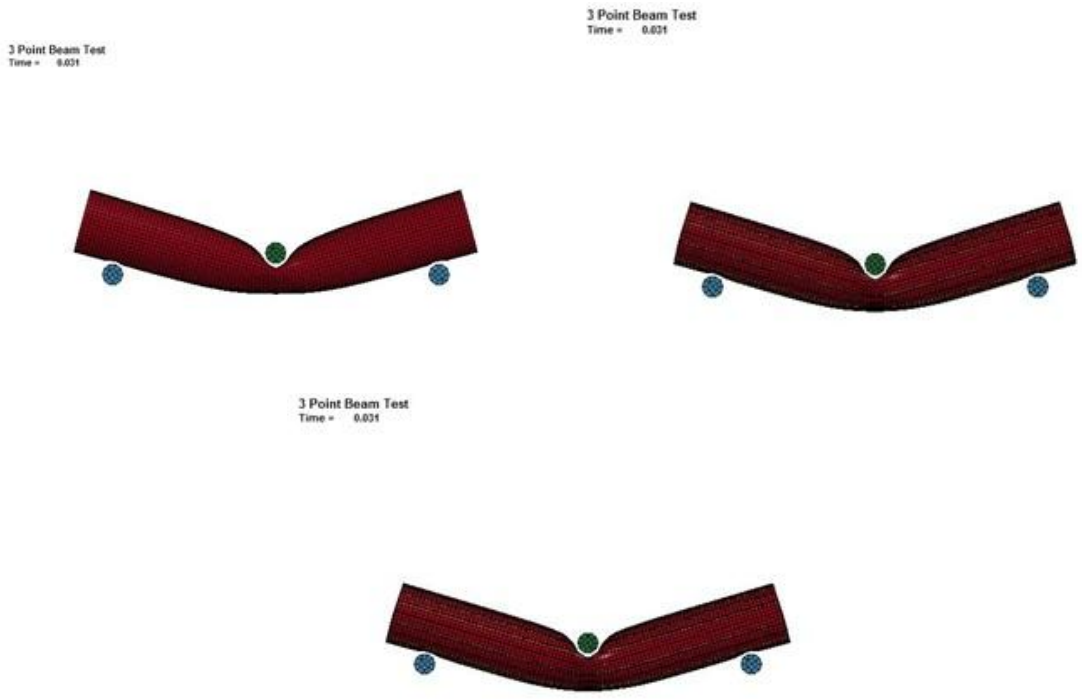

Figure 4.12 Bending test Simulation of Tube with No Foam, With PU and CNF Insert at 0.031sec

CHAPTER 5

ROOF STRENGTH ANALYSIS OF A SPORT UTILITY VEHICLE

The crashworthy simulation has garnered significance and importance in the auto industry as it is less expensive and can yield more information and data than the experimental set up. The FEA software used for these crash simulations is a general practice in the present day and has become an important and integral part of design and development process. In general the crash software should be very sophisticated and advanced to handle different boundary conditions, material models, contact interfaces and large deformations among multiple components and within short duration. LS- DYNA an explicit finite element simulation tool is used to address all the above requirements.

5.1 Finite Element Description of Ford Explorer

The Ford explorer model used in this study was developed by National Crash Analysis Center. (NCAC) is one of the leading research institutes for vehicle highway research and development. In the present study a 2003 Ford Explorer model is utilized to study the energy absorption characteristics of the carbon nanofoam. Researchers from NCAC developed this vehicle model to validate the frontal impact conditions at 30 mph, 35 and 40 mph speeds. The finite element details such as, the number of nodes, elements, number of parts created, number of rigid walls used, etc., are shown in Figure 5.1. The present study is mainly based on the roof strength improvement of a vehicle during rollover. Since the SUV's has more tendency of rollover, this vehicle model has been used. The foam is being modeled into the hollow supporting structures of the vehicle roof and further study is being performed.

Figure 5.1 shows the finite element model of 2003 Ford Explorer. Different mesh sizes were used to reduce the time of simulation. Vehicles generally undergo significant deformation in case of a rollover, hence the top and frontal portions of the vehicle if coarsely meshed.

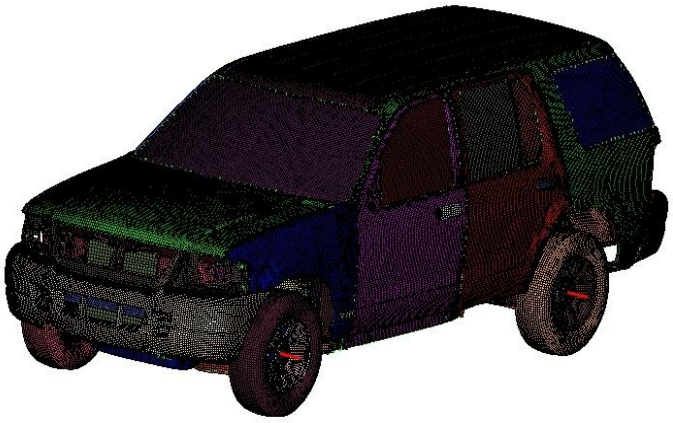

Number of Parts	- 791
Number of Nodes	- 632166
Number of Shells	- 585418
Number of Beams	- 48
Number of Solids	- 33695
Number of Elements	- 619161

Figure 5.1 FE Model of 2003 Ford Explorer [20]

5.2 Finite Element Modeling of Foam Material

The foam is modeled based on the study conducted by Droste, et al [1] to improve the optimal crash performance of a vehicle during frontal crash. In his research, he tried to improve the car body stiffness and crash performance by introducing structural foam as reinforcement to various supporting crashworthy structures of the vehicle, including the roof supporting members. Figure 5.2 shows the possible application areas of structural foam in a vehicle.

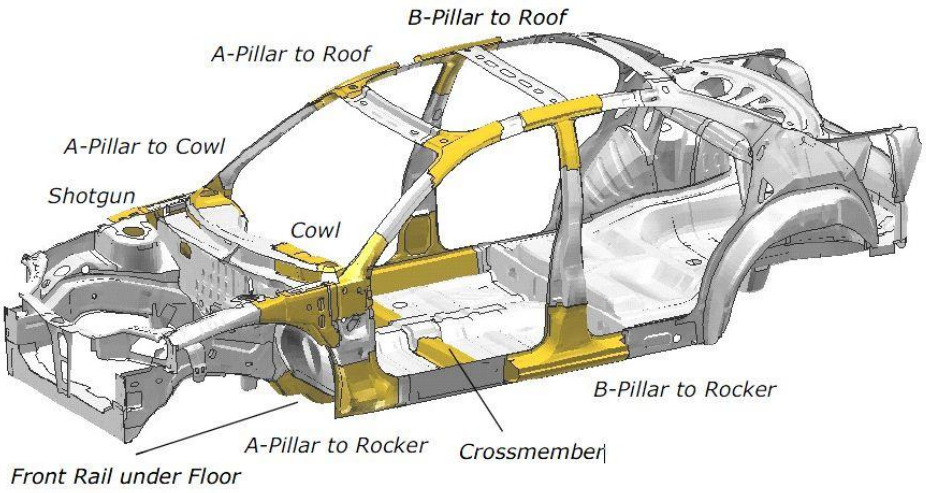

Figure 5.2 Application areas of Structural Foam in a Vehicle [16]

The present study is based on improving the roof strength of a vehicle during a rollover, so the concentration is towards improving the structural performance of roof supporting members. In this

research, the foam material was modeled according to the design of roof supporting components of Ford Explorer. The modeling of foam material is carried on using HYPERMESH. The foam was modeled and inserted into the hollow parts of A- Pillar, B-Pillar, Roof side rail and Roof header, which are commonly known as the roof supporting components. Figure 5.3 and 5.4 shows the finite element model of the foam material being inserted into the vehicle.

Figure 5.3 Modeled Foam according to Hollow Roof Structure Components

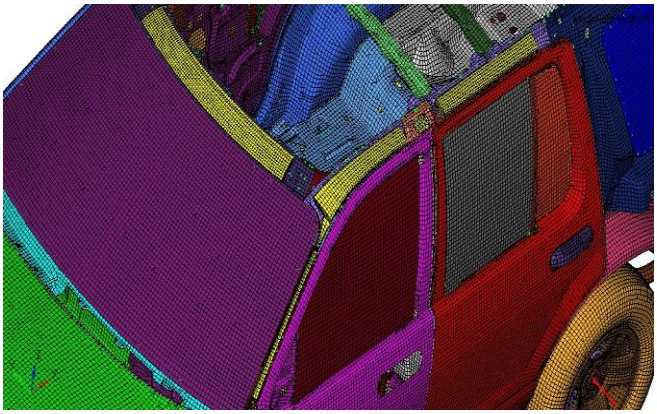

Figure 5.4 Foam Inserted into Hollow Roof Supporting Structure of Ford Explorer

5.2.1 Material and contact modeling

The parameters required for developing the finite element model and the steps involved in the simulation process are carefully done to obtain accurate and efficient model for the study. For the finite element discretization, the foam was modeled using solid element formulation. Since the structural foams

used in the present study i.e., polyurethane foam and carbon nanofoam are crushable with very less recovery, the material card MAT_063 (*MAT_CRUSHABLE_FOAM) is used. Also, the stress hardening and strain rate effects are not considered. The lateral deformation in these types of materials is negligible, due to which the poisons ratio is zero. The material properties used for component level bending simulation in earlier chapters were considered.

A *CONTACT_AUTOMATIC_SURFACE_TO_SURFACE card is defined as a contact interface between the foam material and the structural components. CONTROL_ENERGY card is assigned to the model where hourglass energy is computed and included in the energy balance. To avoid negative volume and error termination in the foam material a *CONTACT_INTERIOR card was assigned. Table 5.1 shows the finite element details of foam model.

Table 5.1 FE Model details of Modeled Foam

Element Length of foam	8mm
Number of Nodes in foam	11091
Number of elements in foam	8666

5.3 Finite Element Analysis of Test Set up

In the present study, Finite element analysis of both static and dynamic cases of rollover i.e. FMVSS 216, a quasi-static roof crush test and SAE J996, a dynamic invert drop test have been considered. The simulations and results in both the conditions for different cases is observed and tabulated. The three important cases for this research are:

- Without foam material
- With polyurethane foam insert
- With carbon nanofoam insert

5.3.1 Quasi static testing – FMVSS 216

The Ford explorer is used for this study as it is a sport utility vehicle and gives a good overview of a rollover scenario. The test set up is shown in Figure 5.5. According to the FMVSS 216 standards, the

load plate is oriented at 25^0 roll angle and 5^0 pitch angles. A complex vector was used to define the path of the load plate movement. In a static test, the weight of the load plate is not involved, so a *MOTION_RIGID_PLATE was considered as the load plate oriented as per the requirements. The load is defined to the rigid load plate in downward direction along the complex vector with no more than 13 mm/sec.

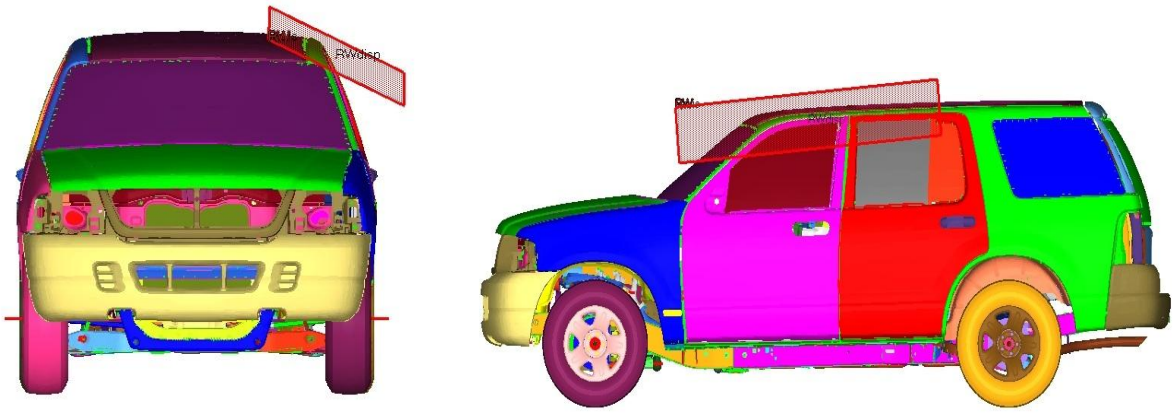

Figure 5.5 FMVSS 216 Test Setup of Ford Explorer

A *BOUNDARY_PRESCRIBED_MOTION_RIGID card is used to define the displacement of the load plate. The contact interface between the load plate and the roof structure, when the load plate exerts a force is defined using *CONTACT_AUTOMATIC_SURFACE_TO_SURFACE card. According to the FMVSS requirements, a fixed contact is assigned between the rigid road surface and the vehicle. In agreement with the quasi static testing standard, a Static force Vs Displacement or roof crush plot is plotted which is also considered as a main criteria for the roof crush resistance compliance in the current study. In order to calculate the static force, *DATABASE_NODFORCE card was used which gives the total and individual force on each node.

5.3.2 Inverted drop testing – SAE J996

In an inverted drop test, the vehicle is hung upside down at 25^0 roll angle and 5^0 pitch angles. According to the test procedure requirements, the vehicle is dropped freely against the gravity on to the

road. Therefore the gravitational acceleration is defined to the vehicle using *LOAD_BODY_Z card. Figure 5.6 shows the Inverted drop test set up.

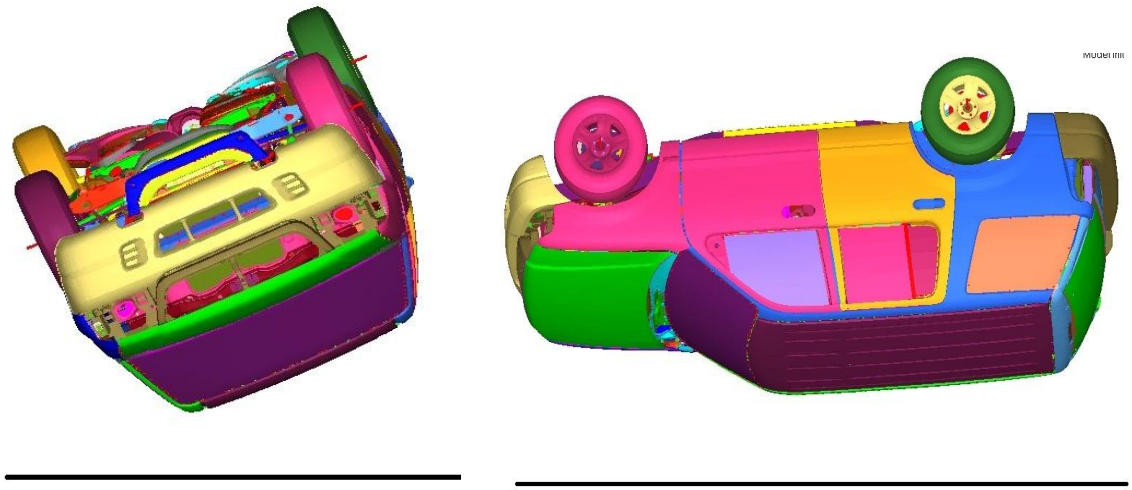

Figure 5.6 SAEJ996 Test Setup of Ford Explorer

A *CONTACT_AUTOMATIC_SURFACE_TO_SURFACE card is used to define the contact interface between the vehicle and rigid floor base. The rigid base force against the nodal displacement at point of impact is plotted using ASCII option in LS- Prepost, same as compared to FMVSS 216.

5.4 Simulation Test Result Comparison

The simulation results for all three conditions i.e, without foam material and with PU foam and carbon nanofoam for both static and dynamic test are observed and tabulated.

5.4.1 Comparison of FMVSS 216 results

The rigid load plate impacts and crush the vehicle roof until the termination time is reached ie, 0.12 sec. The energy absorption characteristics for all the three conditions are observed. Figure 5.7 shows the roof crush at 0.105 seconds.

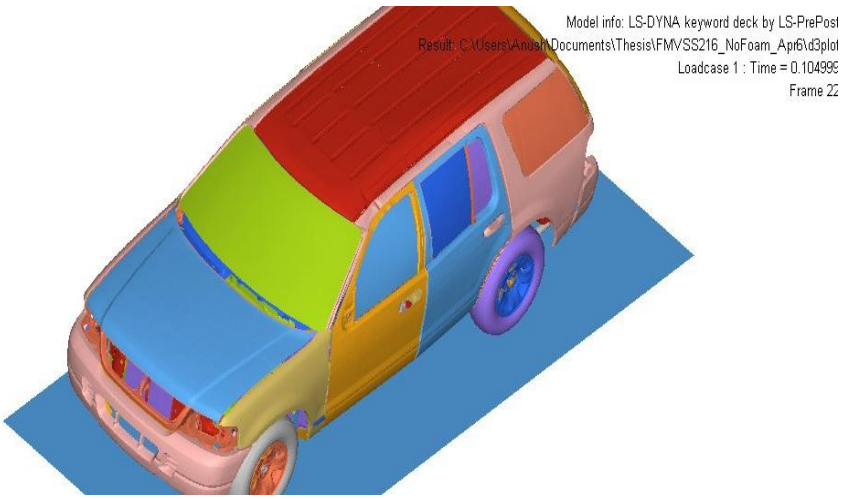

No foam

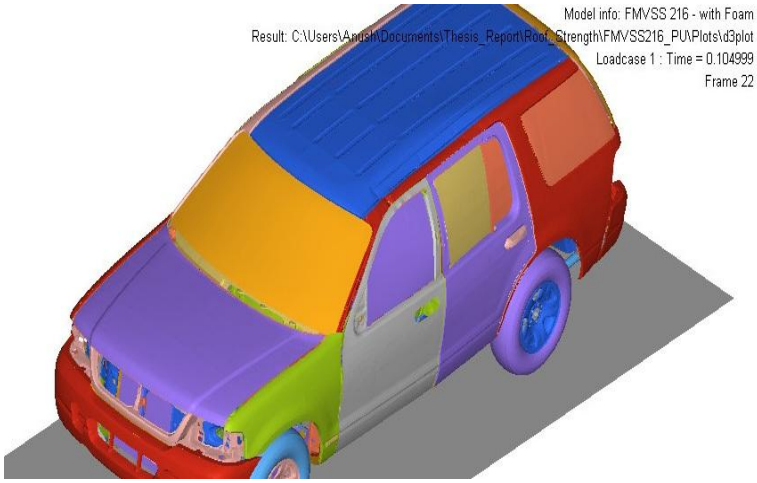

PU Foam

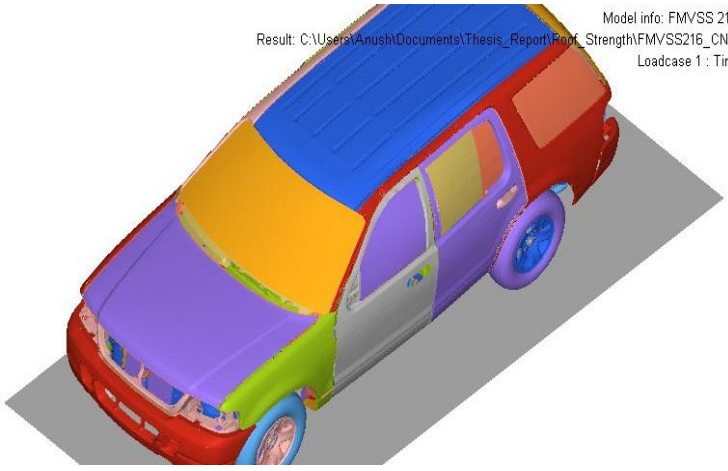

CNF

Figure 5.7 Roof crush of Ford explorer under FMVSS 216 for all three conditions at 0.105 sec

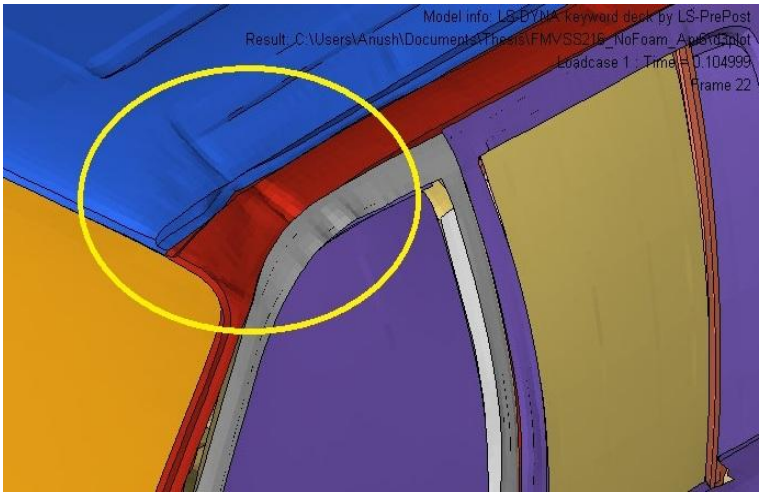

No foam

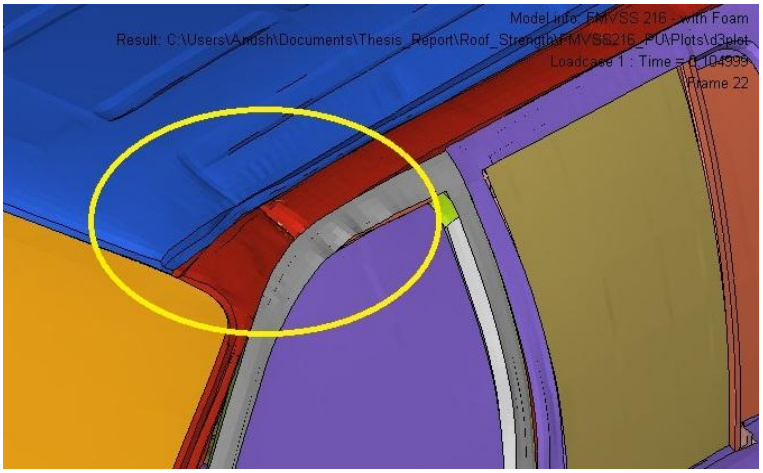

PU Foam

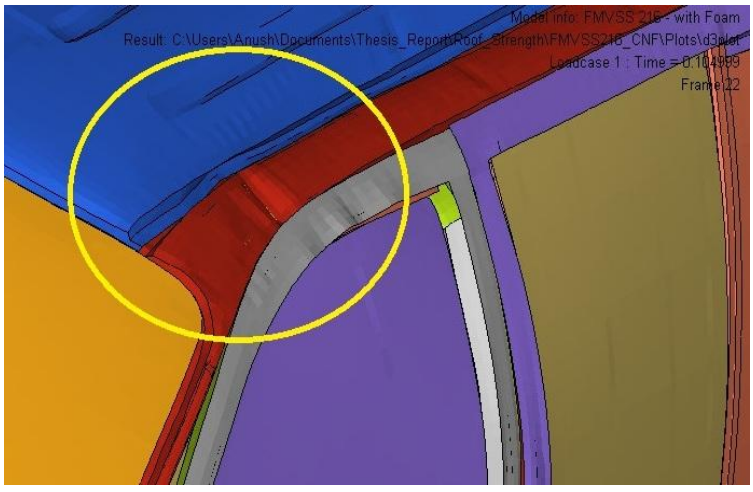

CNF

Figure 5.8 Closer view of roof crush pattern under FMVSS 216 for all three conditions at 0.105 sec

It is clearly observed from Figure 5.8, that the roof deformation pattern of Ford explorer without any foam material is more compared to Ford explorer with polyurethane foam and carbon nanofoam insert. Similarly, the roof deformation is less in Explorer with carbon nanofoam insert compared to that of the Explorer with polyurethane foam insert.

A typical Force vs displacement graph is plotted to study the energy absorption characteristics of the roof at the area of load plate impact to the vehicle. The load plate force against the nodal displacement at the point of impact is plotted using ASCII option in LS- Prepost. All three cases are plotted as shown in Figure 5.9.

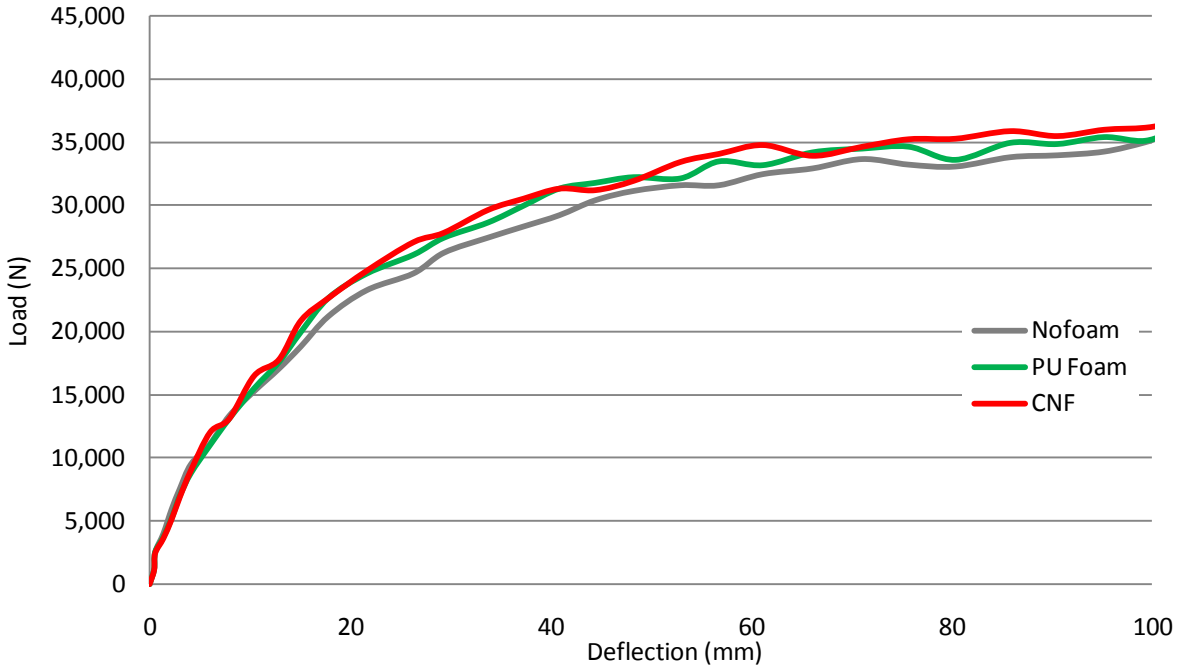

Figure 5.9 Force vs. Displacement Results of FMVSS 216 without Foam, With PU Foam and CNF

According to FMVSS 216 standards, the unloaded vehicle roof should withstand a load of 22,240N, which in this case the ford explorer satisfies the above condition by withstanding a load of 32,500N. The peak loads for all the three conditions vary accordingly as seen in Figure 5.9. It can be observed that the peak load of CNF is more compared to PU foam and unmodified roof structures. Carbon nanofoam exhibits better energy absorption characteristics with maximum peak load of 35800N compared

to explorer without foam material and polyurethane foam with peak loads of 35100N and 34950N. The energy absorption values of vehicle at all three conditions are shown in table 5.2.

Table 5.2 Energy Absorption Characteristics of Roof with and without Foam Insert under FMVSS 216

	Peak load (N)	***% of Increase in Energy***
Unmodified Roof structure	35100 @ 103 mm	Base
Roof structure with Polyurethane foam	34950 @ 85mm	2%
Roof structure with Carbon Nanofoam	35800 @ 86mm	3%

5.4.2 Comparison of SAE J996 results

According to dynamic invert drop testing, the ford explorer is dropped freely on to the ground from a height of 12 inches from the ground. The energy absorption characteristics for all the three conditions are observed. Figure 5.10 shows the roof crush at 0.055 seconds.

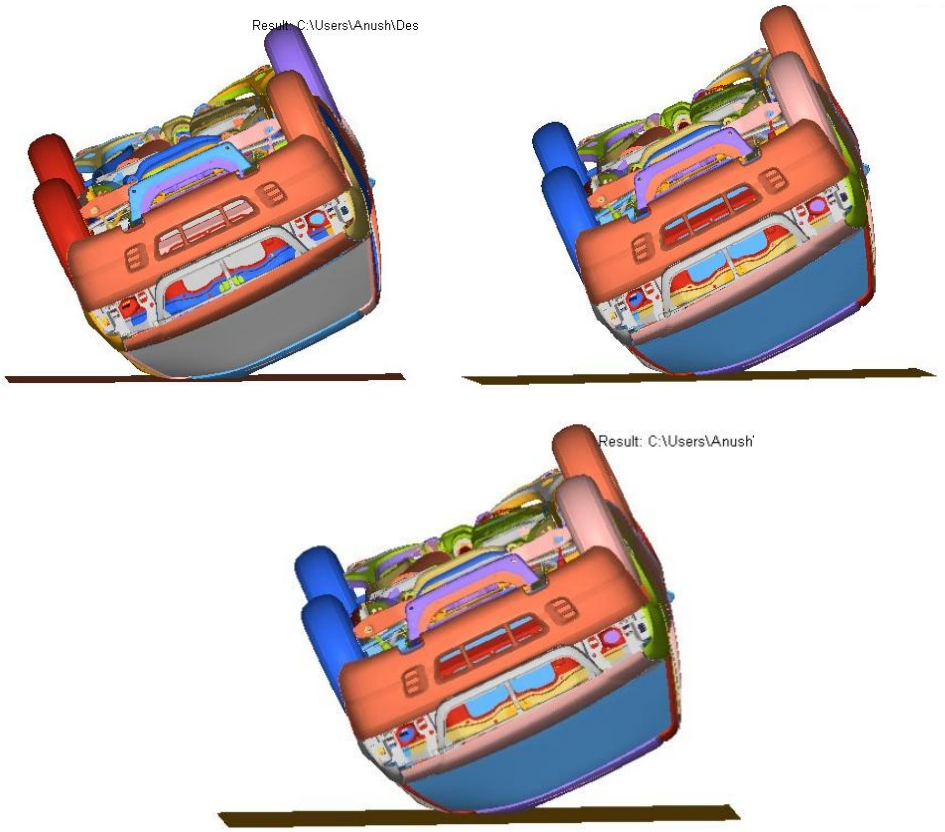

Figure 5.10 Roof Crush of Explorer under SAE J996 without foam, with PU foam and CNF at 0.055 sec

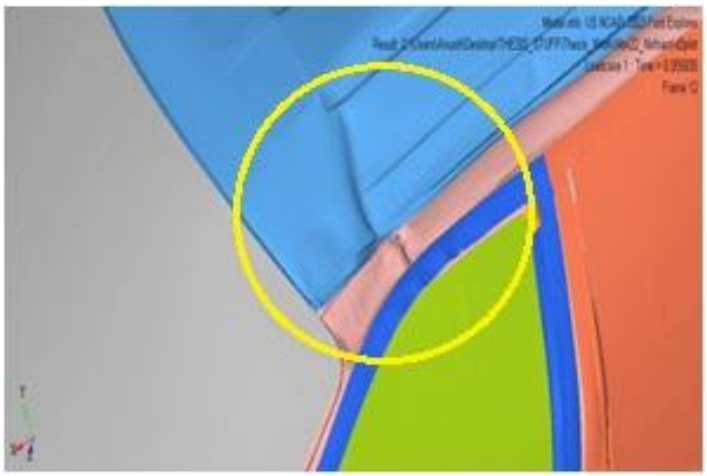

No foam

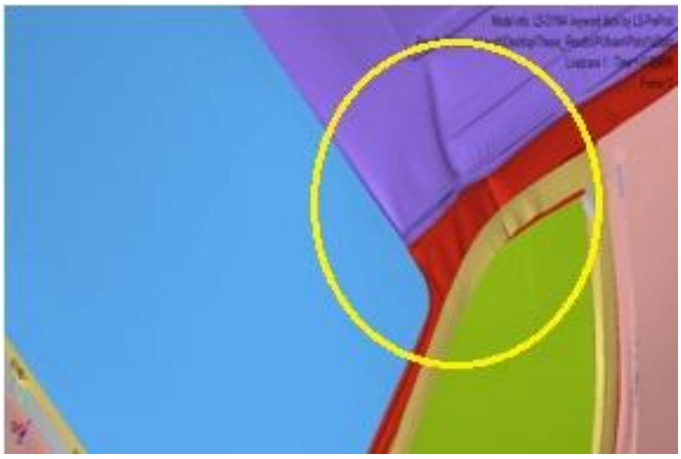

PU Foam

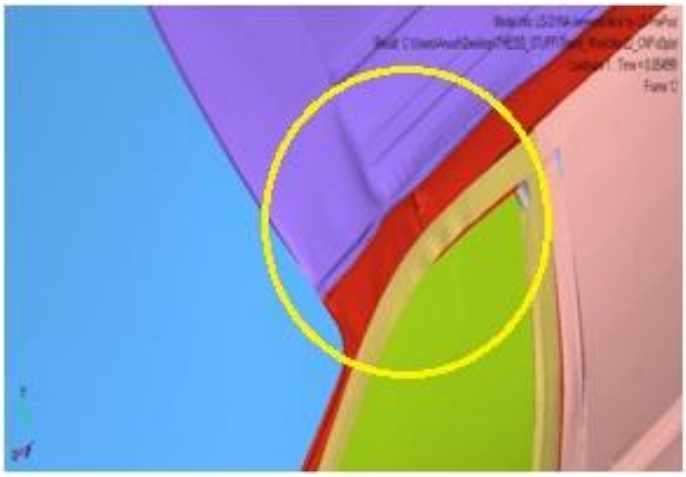

CNF

Figure 5.11 Closer view of Roof Crush pattern of Explorer under SAEJ996 without Foam, with PU foam and CNF insert at 0.055 sec

For better visualization of the deformation near the impact area, zoom in pictures are shown in Figure 5.11. It can be seen that the roof deformation pattern during the drop test of Ford explorer without any foam material is more compared to the explorer with polyurethane foam and carbon nanofoam insert. Similarly, the roof deformation is less in Explorer with carbon nanofoam insert compared to that of the Explorer with polyurethane foam insert.

A Force vs. displacement graph is plotted to study the energy absorption characteristics of the roof at the area of load plate impact to the vehicle. The load plate force against the nodal displacement at the point of impact is plotted using ASCII option in LS- Prepost. The peak loads and energy absorption values of vehicle at three different conditions are observed in Figure 5.12.

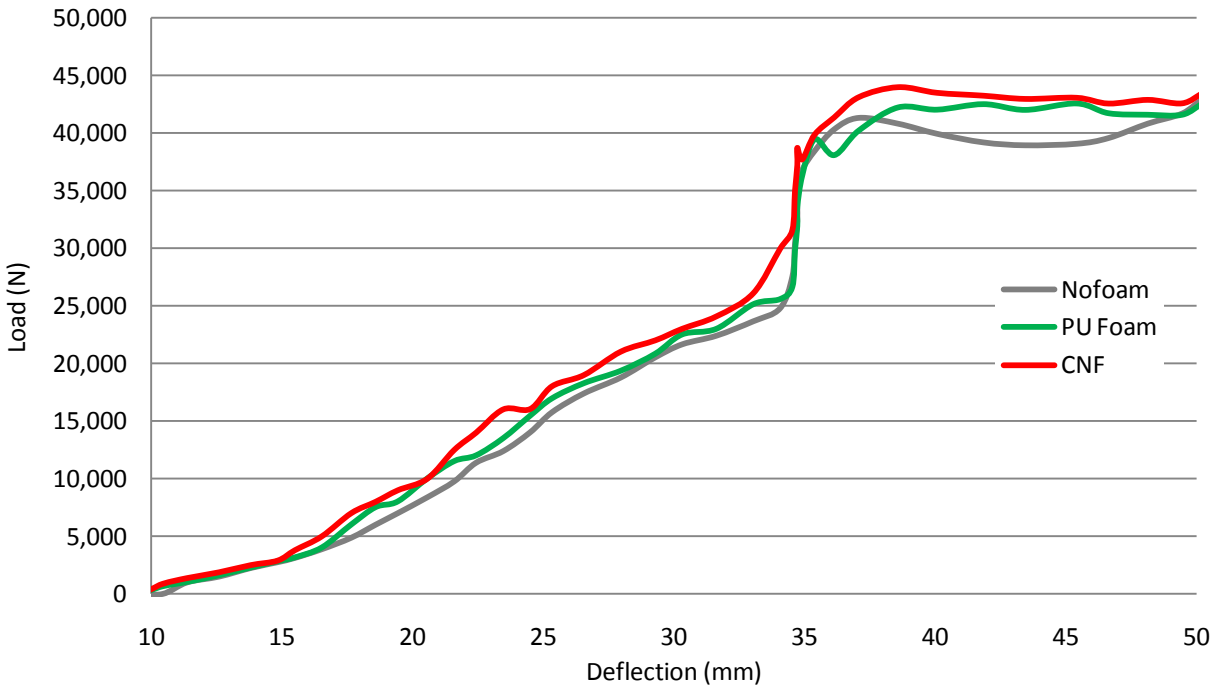

Figure 5.12 Force vs Displacement Results for SAEJ996 without foam, with PU foam and CNF

The peak loads for all three conditions vary accordingly as seen in Figure 5.12. It can be observed that peak load of CNF is more compared to PU foam and unmodified roof structures. Carbon nanofoam exhibits better energy absorption characteristics with maximum peak load of 44000N at 38mm compared to explorer without foam material and polyurethane foam with peak loads of 41400N at 37mm and 42800N at 43.5mm. The energy absorption values of vehicle at all three conditions are shown in table 5.3

Table 5.3 Energy Absorption Characteristics of Roof with and without Foam Insert under SAE J996

	Peak load (N)	***% of Increase in Energy***
Unmodified Roof structure	41400 @ 37 mm	Base
Roof structure with Polyurethane foam	42800 @ 43.5 mm	2%
Roof structure with Carbon Nanofoam	44000 @ 38 mm	3.5%

The increase in energy absorption during the rollover is relatively small with the incorporation of foam material into the hollow roof supporting structures because of the low volume to mass ratio of the foam compared to the huge mass of the vehicle.

5.5 Application Of Nanofoam In Automotive Industry

In 2006, a Nanomaterial Roadmap for 2015 was developed concerning the use of nanomaterials in the automotive sector funded by European commission.

5.5.1 Nanomaterial road map 2015

The nanomaterial road map serves the purpose of giving the small and medium sized enterprises, a concise description of the development in this sector.

The database and the linked roadmap tool were structured, based on several R&Ds, Indutrial SWOT analysis and account of results of European survey on more than 300 European SMEs.

The main purposes of this study are [24]:

- To give an overview of relevant nanomaterials for industrial applications in the automotive sector at short, middle and long term.
- To give the actual level of development of the nanomaterials and an approximate evolution of it at short, middle and long term and to be adapted to SMEs.

Figure 5.13 shows the level of development of nanomaterials and the projection of its evolution in the automotive industry.

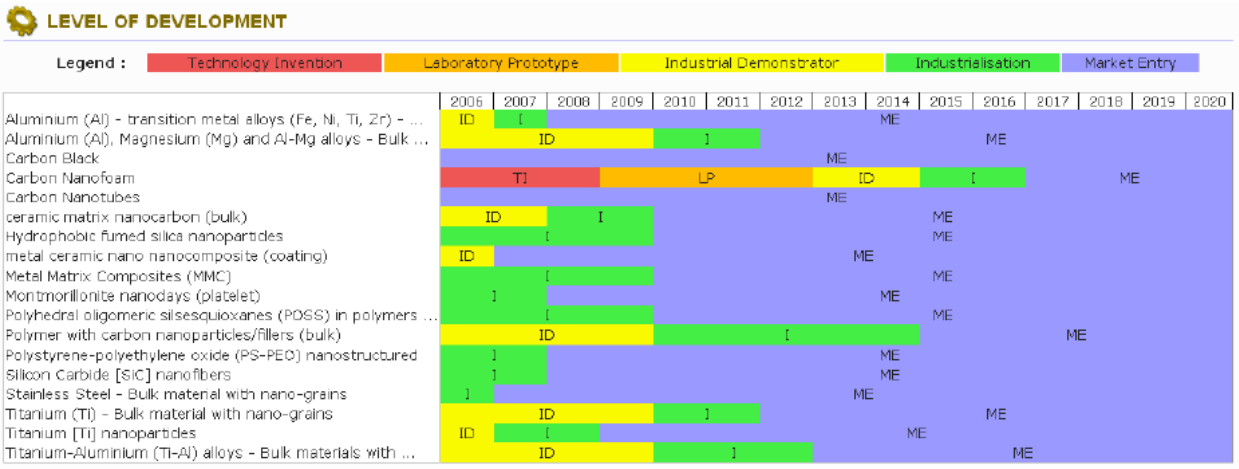

Figure 5.13 Level of Development of Nanomaterials and Projection of its Evolution in Auto Industry [24]

5.5.2 Nanomaterial application in different domains of a car

The report was structured in different domains of a car where, nanomaterials play an important role [24]. The different domains of a car are:

- Frames and Body
- Powertrain and Engines
- Paintings and Coatings
- Suspension and Breaking
- Exhaust Systems
- Electric and Electronic Equipment

The area of concentration of the current thesis is about the application of nanofoam in the structural applications of a vehicle, Therefore Frames and body category is further discussed.

5.5.2.1 Frames and body

The nanomaterials in this domain play an essential role in the future of automotive in overcoming the barriers concerning the industry [24].

- Cost Effectiveness
- Weight Reduction

- Aesthetics
- Recyclability
- Safety and Crashworthiness

Possible solutions through nanomaterials in this domain are:

- Economic light weight parts that improve fuel efficiency
- Vehicle durability could be achieved with CNFs and new metal alloys like Al-Mg/Ti-Mg alloys.
- Nanomaterials or nanocomposites like polymer with nanofillers has advantage of less filler materials required to provide same or improved performance.
- Recyclability and decomposition

5.5.2.2 Development and application of nanomaterials in frames and body domain.

Carbon nanotubes and Nickel (carbon coated) are alredy available in the market. The carbon nanofoam and polymer with carbon fillers would enter the market around 2019 according to experts [24]. Figure 5.14 and 5.15 shows the timeframe for development and nanomaterial application possibility in this sector.

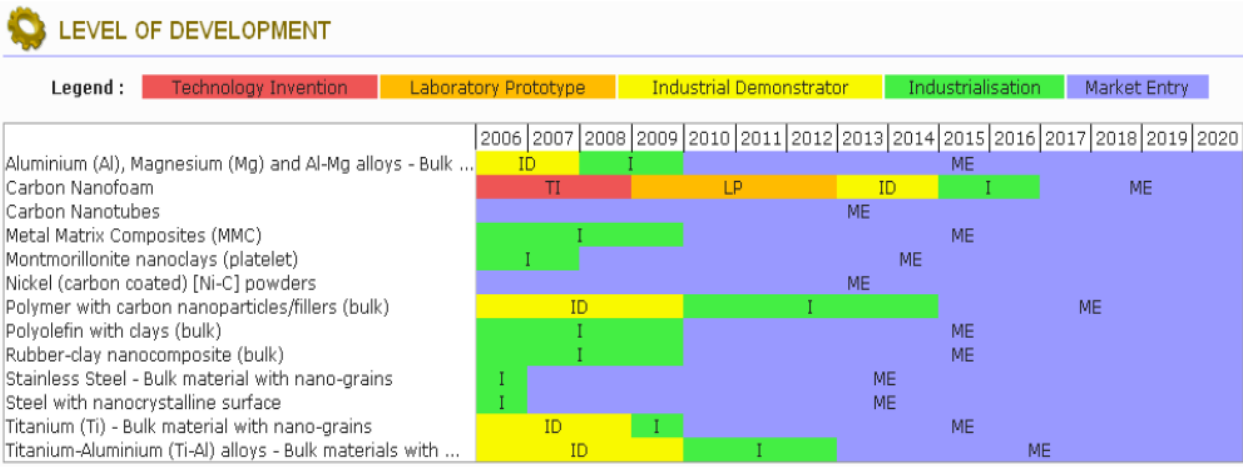

Figure 5.14 Timeframe for Development of the Nanomaterials in Frames and Body Domain [24]

APPLICATIONS

List of specific appplications corresponding to search criteria

	Unspecified	0 - 2 years	3 - 5 years	6 - 10 years
Aluminium (Al), Magnesium (Mg) and Al-Mg alloys - Bulk materials with nano-grains			- Structural material	
Carbon Nanofoam				- Strong lightweight material
Carbon Nanotubes				- Light weight components through foams with carbon nanotubes

Figure 5.15 Nanomaterial Application possibilities in the Frames and Body Domain [24].

The carbon nanotubes market is expected to reach 13billion in the next 5-10 years in the Frames and Body segment, according to experts and surveys as shown in Figure 5.16 and 5.17.

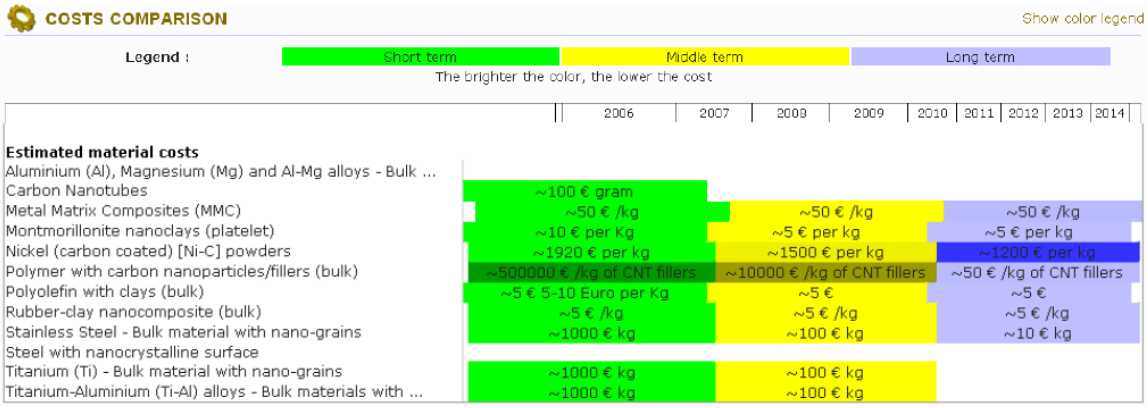

Figure 5.16 Expected costs of Nanomaterials in Frames and Body Segment [24]

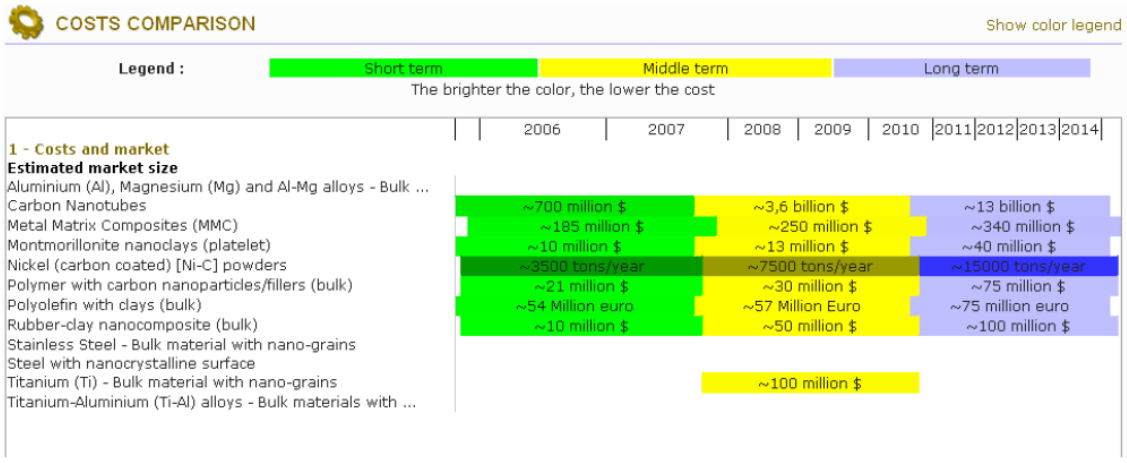

Figure 5.17 Expected Nanomaterials Market size in Frames and Body Segment [24]

Companies already active in this field according to 2006 statistics are General Motors, Toyota, GE Plastics, Bayer AG, Nanocor Inc, Black Hawk automotive plastics Inc, [24]:

CHAPTER 6

CONCLUSIONS AND RECOMMENDATIONS

6.1 Conclusions

In this thesis, a thin walled steel tube was used to study the effects of polyurethane foam and polyurethane foam infused with carbon nanofibers ie, carbon nanofoam on the energy absorption characteristics of the resultant structure. First, component level three point bending test modeling and simulations were carried out on hollow tube and hollow tube with polyurethane foam and carbon nanofoam, to study the effect of foam material on the hollow steel tube. The hollow tube experimental data was used to obtain reasonable correlation data for the numerical model. Non- linear FE models of the tube along with the foam were then developed in LS- DYNA. The FE simulations of the thin walled steel tube filled with polyurethane and with CNF was analyzed and compared with the hollow tube simulation results conducted by Mamalis et al [1]. The application of polyurethane foam and carbon nanofoam in the roof supporting structure area of a Sport utility vehicle was then analyzed.

In this study the effects of polyurethane foam and carbon nanofoam were studied and from the results, the following conclusions are made.

- The CNF foam filled thin walled tube mean load has improved compared to the empty steel tube and steel tube with polyurethane foam.
- The energy absorption capability of the steel tube filled with carbon nanofoam was found to be 30% better than the empty steel tube and 15% better than the steel tube with polyurethane foam.
- The bending behavior due to the impact was observed in steel tube and tube with polyurethane and carbon nanofoam.
- Rollover static and dynamic crash simulations were conducted on the Explorer, to study rollover behavior of the vehicle. The crushing pattern and energy absorption characteristics with and without foam inserts were observed and studied.

- In static FMVSS roof crush testing, the Explorer with CNF foam insert showed improvement in peak loads compared to polyurethane foam insert and without foam, at an increase in energy absorption of 2% and 3%.
- In Dynamic Inverted drop testing, the Explorer with CNF foam insert showed improvement in peak loads compared to polyurethane foam insert and without foam, at an increase in energy absorption of 2% and 3.5%.
- From the simulations and results, it can be concluded that the carbon nanofoam exhibits better energy absorption characteristics compared to polyurethane foam.

6.2 Recommendations for Future Study

Based on the conclusions made in this study, further research can be conducted using carbon nanofoams in various structural applications of automotive, aerospace or in any transportation industry. Some of the primary and significant applications of this thesis work are as follows.

- Producatibility, applicability and cost of utilizing nanofoam inserts as source of energy absorption and further investigation.
- Carbon nanofoam can be applied in the rails and bumpers of the vehicle to study the energy absorption characteristics at different frontal and rear impacts.
- CNF can be applied in the side pillars of a vehicle to study the energy absorption characteristics at different side impacts.
- Head impact and pelvic impact tests can be performed to study the behavior of carbon nanofoam, when used as a padding material in a vehicle.
- Foams also acts as potential source to reduce noise and vibration in a vehicle. Study of CNF as a noise and vibration reducing source would be of interest.

REFERENCES

REFERENCES

[1] Mamalis A.G., Manalakos D.E., Loannidis M.B., Kostazos P.K., "Bending of cylindrical steel tubes: numerical modeling," *International Journal of Crashworthiness,* Vol 11, Issue 1, pp 37-47, 2006.

[2] Poonaya S., Thinvongpituk C., Teeboonma U., " An Analysis of Collapse Mechanism of Thin walled circular tubes subjected to bending", *International Journal of Aerospace and Mechanical Engineering*, 2007.

[3] INSTRON® 3 and 4 point Flexure Fixtures, http://www.instron.us/ [Cited 2012]

[4] Shin -Ken C., Nikolai M., Flavio N., Jihan R., "Vehicle Rollover Avoidance", *Control Systems, IEEE,* Vol: 30, Issue: 4, pp 70-85, Aug 2010.

[5] De Lima A., Marczak R., "Computational Methodologies for Vehicle roof strength assessment in rollover crashes," *Department of Mechanical Engineering* – UFRGS.

[6] Auto accident facts, http://carblackbox4you.com/car-black-box/car-accident-facts/ [Cited 2012]

[7] Tankara D., "Study of the Energy Absorption Characteristics of a Thin walled Tube Filled with Carbon Nano Polyurethane Foam", MS Thesis, Wichita State University, USA 2011.

[8] The physics of SUV Rollover Accidents, http://mb-soft.com/public/rollover.html [Cited 2012]

[9] Asay A.F., Woolley R.L., "Rollover Testing of the Sport utility Vehicle (SUVs) on an Actual Highway," SAE International, DOI: 10.4271/2010-01-0521, Apr 2010.

[10] Slik, G., Vogel, G., Chawda, V., "Material validation of a high efficient energy absorbing foam," 5th Ls-Dyna Forum, Material III Foams/Composites, Dow Automotive, Materials Engineering Center, Germany, 2006.

[11] Sandeep C.K., "Thermoplastic Roof crush countermeasure design for improved Roof cruch Resistant to meet FMVSS 216", *SAE International*, DOI: 10.4271/2011-01-1119, Apr 2011.

[12] Bio mechanics of Rollover Accidents, http://www.synapacg.com/feature.html [cited 2012]

[13] Vehicle Structural areas prone to accidents, http://www.subaruofkeene.com/why_subaru.htm [cited 2010]

[14] Kallina I., Zeidler F., Baumann K.H., Scheunert D., "The Offset Crash against a Deformable Barrier, A more Realistic Frontal Impact," *Proceedings of the 4th International Technical Conference on Enhanced Safety of Vehicles*, Munich, Germany, May 1994.

[15] Shigeaki K., Guoxing L., Dong R., John B., "Experimental and FE analysis of Quasi- Static bending of foam – filled structures," SAE International, April 2010.

[16] Droste A., Jan R., "Crash peroformance Increase with Structural BETAFOAM," 6th LS-DYNA Forum, Dow Automotive, Schwalbach, Germany 2007.

[17] Basics of Duocel® foams, http://www.ergaerospace.com/Descriptors.htm, technical data and properties [cited 2011]

[18] Saha, M.C., Kabir, Md.E., Jeelani, S., "Enhancement in thermal and mechanical properties of polyurethane foam infused with nanoparticles," *Material Science and Engineering*, Vol 479, Issues 1-2, pp 213-222, April 2008.

[19] US Department of Transportation. "National Highway Trafic Safety Administration, "Laboratory test procedure for FMVSS 216, Roof Crush Resistance," TP-216-05, Nov 2006.

[20] "Finite Element Model of Ford Explorer," NHTSA National Crash Analysis Center (NCAC), Version 2, 2003.

[21] Shenoy S.S., "Energy Absorption of a Car Roof Reinforced with Grid Stiffened Composite Panel in the Event of a Rollover," MS Thesis, Wichita state University, USA 2002.

[22] "Introduction to Finite Element Methods," *Department of Aerospace Engineering Sciences*, ASEN 5007, University of Colorado at Boulder, Fall 2012

[23] "Stress and Strains in a Three Point Loaded Beam," *Department of Mechanical Engineering*, ME 354, Lab1- Worksheet, University of Washington, USA.

[24] "Roadmap Report Concerning the Use of Nnaomaterials in the Automotive Sector," *Nanomaterial Roadmap 2015,* Sixth Framework Program, 2006.